



WILLIAM LETTIS & ASSOCIATES, INC.

## Final Technical Report

# Paleoseismology of a Secondary Strand of the Central Calaveras Fault in Halls Valley, Santa Clara County, California



Prepared for:  
U.S. Geological Survey  
National Earthquake Hazards Reduction Program  
Award No. 03HQGR0098

Prepared by:  
William Lettis & Associates, Inc.  
1777 Botelho Drive, Suite 262  
Walnut Creek, CA 94596

June 2004



**FINAL TECHNICAL REPORT**

**PALEOSEISMOLOGY OF A SECONDARY STRAND OF THE CENTRAL CALAVERAS  
FAULT IN HALLS VALLEY, SANTA CLARA COUNTY, CA**

**Recipient:**

William Lettis & Associates, Inc.,  
1777 Botelho Dr., Ste. 262, Walnut Creek, CA 94596  
Phone: (925) 256-6070; Fax: (925)256-6076  
URL [www.lettis.com](http://www.lettis.com)

**Principal Investigators:**

Robert C. Witter, Keith I. Kelson, and Sean Sundermann  
E-mail: [witter@lettis.com](mailto:witter@lettis.com)

**Program Elements I and II**

**Keywords:**

Paleoseismology, Geologic Mapping, Surficial Deposits, Tectonic Structures

U. S. Geological Survey  
National Earthquake Hazards Reduction Program  
Award Number 03-HQ-GR-0098

June 2004

Research supported by U.S. Geological Survey (USGS), Department of Interior, under USGS award number 01HQGR0098. The views and conclusions contained in this document are those of the authors and should not be interpreted as necessarily representing the official policies, either expressed or implied, of the U.S. Government.

## **TABLE OF CONTENTS**

---

Abstract .....	iv
1.0 Introduction.....	1
2.0 Seismotectonic Setting.....	2
3.0 Fault-related Geomorphology of Halls Valley Site .....	5
4.0 Evidence of Aseismic Creep at Halls Valley .....	6
5.0 Subsurface Trenching Investigation of Secondary Fault .....	7
5.1 Approach and Methods.....	7
5.2 Estimates of Deposit Age .....	7
5.3 Near-Surface Stratigraphy .....	7
5.4 Near-Surface Structural Relationships .....	9
5.4.1 Eastern Fault Strand .....	9
5.4.2 Western Fault Strand.....	11
6.0 Discussion.....	12
6.1 Possible Evidence for Surface Fault Rupture and Implications for Seismic Hazard.....	12
6.2 Slip History of Secondary Faults in Halls Valley.....	13
6.3 Possible Explanations for Reverse Faults in Halls Valley.....	13
7.0 Summary of Findings.....	15
8.0 Acknowledgments.....	17
9.0 References.....	18

## **LIST OF TABLES**

---

Table 1. Historical seismicity greater than M 5.0 along the central Calaveras fault .....	2
---	---

## **LIST OF FIGURES**

---

- Figure 1. Shaded relief map of the major active faults in the southern San Francisco Bay region.
- Figure 2. Simplified map of active traces of the central Calaveras fault, showing previous sites of paleoseismic investigation, existing creep measurements sites and the Halls Valley study site.
- Figure 3. Map of central Calaveras fault and associated instrumental seismicity from Northern California Earthquake Data Center and Schaff et al. (2002).
- Figure 4. Quaternary geologic and geomorphic map of the central Calaveras fault at Halls Valley (Witter et al., 2003).
- Figure 5. Interpreted aerial photograph of Halls Valley showing study site and possible fault-related geomorphic lineaments (red) and tectonic depressions (blue).

- Figure 6. (A) Oblique aerial photograph of trench site looking southwest showing the north trending linear trough, northwest-trending tonal lineaments (white arrows), possible tectonic depressions containing vernal ponds, and apparently undeformed historic fenceline. (B) Photograph facing east that shows straight historic fenceline apparently undeformed by creep on secondary traces of the central Calaveras fault.
- Figure 7. (A) Photograph of Halls Valley trench site looking east toward Mt. Hamilton in the distance. (B) Photograph of Halls Valley trench site looking west.
- Figure 8. (A) Photograph (looking north) showing the Halls Valley trench site, northwest-trending tonal lineaments (black lines) and two vernal ponds within a north-trending linear depression. (B) Detailed topographic map of trench site showing the orientations of two northwest-striking, northeast-dipping reverse faults observed in trench.
- Figure 9. Log of south wall of exploratory trench.
- Figure 10. Detailed log of eastern reverse fault exposed in south wall of trench.
- Figure 11. Detailed logs of eastern and western fault strands.
- Figure 12. (A) Oblique photograph from within trench of the eastern fault strand exposed in south wall. (B) Closeup photograph showing slickensides on fault plane.
- Figure 13. (A) Map of fault-related geomorphic lineaments that define a right-releasing stepover along the central Calaveras fault at Halls Valley. (B) Interpreted map of faults and pull-apart basin (green area) formed by a scaled sandbox experiment designed to model releasing stopovers along strike-slip faults (Dooley and McClay, 1997).

Award No. 03HQGR0098

**PALEOSEISMOLOGY OF A SECONDARY STRAND OF THE CENTRAL CALAVERAS  
FAULT IN HALLS VALLEY, SANTA CLARA COUNTY, CA**

Robert C. Witter, Keith I. Kelson and Sean Sundermann

William Lettis & Associates, Inc.  
1777 Botelho Drive, Suite 262; Walnut Creek, CA 94596  
Phone: (925) 256-6070; Fax: (925) 256-6076  
E-mail: [witter@lettis.com](mailto:witter@lettis.com)

**ABSTRACT**

---

The late Holocene rupture behavior of the rapidly creeping central Calaveras fault remains poorly defined despite recent probabilistic hazard assessments that forecast an 11% probability of one or more large,  $M \geq 6.7$  earthquakes on the Calaveras fault between 2002 and 2031. The uncertainty arises from conflicting data sets over different time scales. Historical seismicity indicates that the strain budget may be accounted for entirely by aseismic creep and moderate-magnitude ( $M$  5.1 to 6.2) earthquakes. However, geologic investigations at San Ysidro Creek document multiple late Holocene alluvial channels displaced by the fault that have been interpreted as evidence for surface fault rupture produced by  $M \geq 6.2$  earthquakes. This study investigates the hypothesis that the central Calaveras fault only releases strain through aseismic creep and moderate-magnitude ( $M \leq 6.2$ ) earthquakes and not larger ( $M \geq 6.2$ ) earthquakes that may produce surface fault rupture. Our approach involved trenching across a series of secondary faults that are oriented obliquely to the regional fault strike and show no sign of historical creep. The purpose of trenching was to evaluate the presence or absence of geologic evidence for surface fault rupture on the secondary faults that would refute or confirm the hypothesis, respectively.

Our results document evidence for reverse displacement on two faults that strike N 20° to 40° W and dip 47° to 56° NE. Slickensides on the fault planes indicate pure dip-slip movement and vertical separation of late Pleistocene to early Holocene strata indicates reverse displacement. Possible evidence for surface fault rupture during the most recent earthquake includes a proximal colluvial wedge, multiple upward-terminating fault strands, and evidence for high erosion rates that would likely outpace a much slower rate of scarp growth produced by a vertical component of aseismic creep. Based on the probable age of the colluvial wedge and offset of a buried soil, respectively, we interpret that the scarp records early to middle Holocene surface rupture with 0.4 to 0.6 m of displacement. Increasing amounts of reverse displacement and eastward tilting of alluvial strata with depth suggest multiple events. The lack of diagnostic features produced by surface rupture during earlier episodes of deformation precludes a definitive assessment of whether fault movement prior to the most recent event involved surface rupture or creep. However, we interpret that trench exposures may record 0.4 to 1.1 m of reverse slip per event produced by two or possibly three earthquakes. The trench contains no conclusive evidence of creep. We propose two possible explanations for secondary reverse faults located near an extensional stepover along the central Calaveras fault at Halls Valley: (1) analog models of pull-apart basins show that secondary reverse faults, similar to the faults studied here, evolve near the ends of extensional stepovers along strike slip faults due to complex fault interactions; and (2) contractional deformation may be related to the transfer of slip between the central Calaveras and southern Hayward faults. Our data do not distinguish the validity of either explanation.

If correct, our interpretation that Holocene surface fault rupture has occurred on secondary faults along the central Calaveras fault refutes the hypothesis that strain is only accommodated by creep and moderate-magnitude ( $M$  5.1 to 6.2) earthquakes and allows the possibility that future earthquakes may

exceed **M** 6.2. The results of this study, although not definitive, emphasize the need for additional geologic investigations of the various modes of strain release along the central Calaveras fault. Because it poses substantial earthquake-related hazards to the heavily urbanized Santa Clara valley, future probabilistic assessments should continue to evaluate the seismic potential of the central Calaveras fault.

## 1.0 INTRODUCTION

---

The 142-km-long, historically active Calaveras fault zone, a major component of the San Andreas fault system, poses significant earthquake hazards to the densely populated San Jose and San Ramon urban centers (Figure 1). The Working Group on California Earthquake Probabilities (WGCEP, 2003) forecasts an 11% probability of one or more large,  $M \geq 6.7$  (where  $M$  is moment magnitude) earthquakes on the Calaveras fault between 2002 and 2031. Despite their assessment, the late Holocene rupture behavior of the rapidly creeping central and southern segments of the fault remains poorly known and contributes large uncertainty to probabilistic hazard assessments. Historically, strain release along the central Calaveras fault, the focus of this investigation, has occurred through aseismic slip (creep) and several moderate-magnitude ( $M$  5.1 to 6.2) earthquakes (Figure 2). However, trench exposures near San Ysidro Creek (Baldwin et al., 2002; Kelson et al., 1998) contained geologic relationships that have been interpreted as evidence for surface fault rupture. These data leave open the possibility that large earthquakes have ruptured the central Calaveras fault at least three times since the middle Holocene.

Additional uncertainty in the seismic potential of the Calaveras fault arises from the complex transfer of slip between the central Calaveras fault and the southern Hayward fault. The southern Hayward fault inherits  $9 \pm 2$  mm/yr of slip (WGCEP, 2003) from the Calaveras fault near the boundary between the northern and central Calaveras faults (Figure 2). This slip transfer is consistent with a concomitant northward decrease in the slip rate between the central Calaveras ( $15 \pm 3$  mm/yr) and northern Calaveras ( $6 \pm 2$  mm/yr) faults (WGCEP, 2003). A series of northwest-trending oblique-reverse faults that bound the eastern Santa Clara Valley, including the Warm Springs, Evergreen and Quimby faults, are aligned with the southern termination of the Hayward fault and may accommodate transpressional strain related to the left-restraining geometry between the central Calaveras and southern Hayward faults (Aydin and Page, 1984; Ellsworth et al., 1982; Graymer, 1995; Fenton and Hitchcock, 2001). Aligned seismicity bands that trend sub parallel to the southern Hayward fault near Alum Rock and Mission Peak (Figure 3) corroborate evidence for westward slip transfer between the central Calaveras and southern Hayward faults (Andrews et al., 1993).

This investigation was designed to test the hypothesis that the central Calaveras fault only releases strain through aseismic creep and moderate ( $M \leq 6.2$ ) earthquakes and not large ( $M \geq 6.2$ ) earthquakes that may produce surface fault rupture. To test the hypothesis, we investigated a series of secondary faults that lacked evidence for aseismic creep noted during previous detailed geologic mapping of the active traces of the central Calaveras fault (Witter et al., 2003). If geologic evidence shows that secondary faults not subject to creep instead reflect surface fault rupture, then we would reject the null hypothesis stated above and conclude that the central Calaveras fault accommodates strain also by large ( $M \geq 6.2$ ) earthquakes. Our study site lies within Halls Valley, a small fault-controlled pull-apart basin in the Diablo Range east of San Jose, California (Figure 1). The trench site in Joseph D. Grant County Park crosses a north-trending linear trough that defines the northwestern boundary of a 1- to 1.5-km-wide releasing stepover in the central Calaveras fault zone that forms Halls Valley (Figure 4). Within the linear trough is a series of secondary faults that shows no evidence for historic aseismic creep and may be locked. Thus, the fault-related landforms may not be related to creep, but instead, may be products of earthquakes that ruptured the ground surface. Although we observed no evidence for historical offset of cultural features that cross the secondary faults investigated by this study, measurements of a local geodetic array indicate that historical creep occurs on faults that bound the eastern and western margins of Halls Valley (Prescott et al., 1984). These data leave open the possibility that the behavior of the central Calaveras fault zone is not limited to aseismic creep, and that late Holocene geomorphic features along secondary faults may record surface fault rupture.

## 2.0 SEISMOTECTONIC SETTING

Abundant microseismicity and several historic moderate-magnitude earthquakes (Figure 3; Table 1) characterize the historic modes of strain release on the central Calaveras fault (Bakun, 1980; Bakun, 1984; Bakun and Lindh, 1985; Cockerham and Eaton, 1987; Oppenheimer et al., 1990; Schaff et al., 2002). Analyses of the spatial distribution of microseismicity before and after historic moderate earthquakes shows that fault deformation occurs through aseismic creep above 5 km depth, combined creep and microearthquakes at depths between 5 and 10 km, and  $M \geq 5$  earthquakes at depths between 8 and 10 km (Oppenheimer et al., 1990). Between 1949 and 1988, four consecutive  $M > 5$  earthquakes ruptured the fault in a northward progression as post-seismic relaxation following one event triggered the next event (Du and Aydin, 1992). The earthquake cycle proceeded from south to north as follows (Figure 3): 1949 Gilroy earthquake ( $M$  5.2); 1979 Coyote Lake earthquake ( $M$  5.9); 1984 Morgan Hill earthquake ( $M$  6.2); and ended with the 1988 Alum Rock earthquake ( $M$  5.1) (Oppenheimer et al., 1990). The Coyote Lake and Morgan Hill rupture areas appear to have slipped previously in 1897 and 1911, respectively (Oppenheimer et al., 1990; Topozada and Parke, 1982; Topozada et al., 1981).

**Table 1. Historical seismicity greater than  $M$  5.0 along the central Calaveras fault**

Date	Mag	Latitude	Longitude	Depth	Name	Reference
20 Jun 1897	6.2	37°N 00'	121°W 30'	n.d.	Unnamed	Topozada et al., 1981
6 Jul 1899	5.8	37°N 12'	121°W 30'	n.d.	Unnamed	Topozada et al., 1981
1 Jul 1911	6.5	37°N 18.5'	121°W 40.7'	~8.5	Morgan Hill	Oppenheimer et al., 1990
26 Oct 1943	5.1	37°N 23.22'	121°W 44.59'	8.55	Alum Rock	Oppenheimer et al., 1990
9 Mar 1949	5.2	37°N 01.2'	121°W 28.8'	n.d.	Gilroy	Bolt and Miller, 1975
5 Sep 1955	5.5	37°N 22.2'	121°W 46.8	n.d.	Unnamed	Bolt and Miller, 1975
6 Aug 1979	5.9	37°N 06.24'	121°W 31.07'	8.95	Coyote Lake	Oppenheimer et al., 1990
24 Apr 1984	6.2	37°N 18.56'	121°W 40.68'	8.42	Morgan Hill	Oppenheimer et al., 1990
31 Mar 1986	5.7	37°N 28.17'	121°W 41.63'	8.54	Mt. Lewis	Oppenheimer et al., 1990
13 Jun 1988	5.1	37°N 23.22'	121°W 44.59'	8.55	Alum Rock	Oppenheimer et al., 1990

Two prominent trends of instrumentally recorded seismicity depart from the central Calaveras fault and appear to be associated with slip partitioning from the central Calaveras fault northwest onto the southern Hayward fault (Figure 3). The Alum Rock seismicity trend, which is oriented between N45°W to N50°W, diverges northwestward at Halls Valley where dense seismicity concentrated on the central Calaveras fault trends about N35°W (Figure 3). The WGCEP (2003) defines the southern termination of the Hayward fault to be halfway between the southern end of the 1868 surface rupture at Agua Caliente Creek and the Alum Rock seismicity trend. The Mission seismicity trend departs from the northern end of the central Calaveras fault at Calaveras Reservoir, continuing to the northwest (N50°W) where it intersects the southern Hayward fault near the town of Fremont (Figure 3). Andrews et al. (1993) suggested that the Mission seismicity trend reflected a left-restraining stepover between the central Calaveras and southern Hayward faults. Reverse-faulting focal mechanisms along the trend are consistent with this interpretation (Wong and Hemphill-Haley, 1992). Several workers postulate that reverse and/or

thrust faults, such as the Evergreen, Quimby, and Silver Creek faults accommodate contraction related to slip transfer between the Calaveras and Hayward faults (Ellsworth et al., 1982; Aydin and Page, 1984; Fenton and Hitchcock, 2001). The Alum Rock and Mission seismicity trends accommodate the transfer of about 9 mm/yr of northwest-oriented slip (WGCEP, 2003) between the central Calaveras fault and the southern Hayward fault. The left-restraining geometry of this slip transfer produces contraction and uplift of the Diablo Range, which appears to be activating several northeast-dipping reverse faults between the central Calaveras and southern Hayward faults.

Rates of aseismic creep on the central Calaveras fault vary along the length of the segment and through time. A progressive decrease in the rate of creep along the fault, from south to north, has been observed by repeated measurements of a USGS alignment array near Coyote Lake (Coyote Ranch array), and intermittent measurements of two trilateration networks at Halls Valley and Calaveras Reservoir (Figure 2). The Coyote Ranch array shows an average creep rate of 17 mm/yr over a period of 32.7 years (1968-2001), the highest creep rate recorded in the San Francisco Bay region (Galehouse and Lienkaemper, 2003). Between Coyote Lake and Halls Valley the rate of creep decreases to about 9 mm/yr (Prescott et al., 1984). Between Halls Valley and Calaveras Reservoir the creep rate declines, in turn, from about 9 mm/yr to  $2.2 \pm 0.5$  mm/yr, the latter rate estimated from 1970 to 1980 (Prescott et al., 1981). Measurement of an alignment array near the southern end of the central Calaveras fault (at Furtado Ranch, 12 km south of the Coyote Ranch array) shows a creep rate of 15 mm/y over the past 30 years (Kelson et al., 2003).

The only late Holocene geologic slip rate estimate on the central Calaveras fault comes from paleoseismic investigations at the San Ysidro Creek site about 5 km southeast of the Coyote Ranch array. Baldwin et al. (2002) and Kelson et al. (1998) excavated five fault-normal and six fault-parallel trenches across the primary active trace of the fault that exposed six to eight offset stream channels. Measurements of cumulative right-lateral displacement of the oldest four paleochannels provide a middle-to-late Holocene slip rate estimate of 8 to 19 mm/yr (Baldwin et al., 2002). Within the uncertainty of the geologic data, the long-term slip rate estimate is compatible with short-term slip rates derived from aseismic creep data and geodetic modeling. In addition, these data were interpreted as evidence for three earthquakes that ruptured the ground surface between 2000 and 4000 years ago (Kelson et al., 1998).

Uncertainties in probabilistic hazard assessments for the Calaveras fault are strongly influenced by estimates of the maximum earthquake magnitude and rupture behavior of the central and southern fault segments (WGCEP, 2003). Previous hazard assessments assigned a maximum magnitude of  $M$  6.2 for the central Calaveras fault (WGNCEP, 1996) based on the agreement between the geodetic/creep rates and the regional slip-rate budget (Kelson et al., 1992a) that suggests that the fault accumulates little elastic strain. However, more recent earthquake hazard assessments (WGCEP, 2003) consider scenarios that allow large ( $M > 6.2$ ) earthquake ruptures of multiple segments including the central Calaveras fault. WGCEP (2003) included models with large magnitude ruptures because trench exposures across the fault at San Ysidro Creek showed geologic relations that have been interpreted as evidence for large earthquakes capable of surface fault rupture (Baldwin et al., 2002; Kelson et al., 1998). By weighting various fault-rupture models, which included scenarios of both moderate and large earthquakes, the WGCEP (2003) incorporated the uncertainties resulting from incomplete knowledge of long-term fault behavior. Through this approach, the WGCEP (2003) determined that the uncertainty in maximum earthquake magnitude on the central Calaveras fault contributed significant uncertainty in the probability estimates.

Other than the recent research at San Ysidro Creek (Baldwin et al., 2002; Kelson et al., 1998), additional evidence for large earthquakes ( $M \geq 6.5$ ) has not been conclusively demonstrated along the central or southern sections of the Calaveras fault. Following the work at San Ysidro Creek, Stenner et al. (1999) excavated two trenches at a site on the southern Calaveras fault near Hollister, in part to address the

question raised at the San Ysidro Creek site. These workers noted that there was insufficient evidence to determine whether late Holocene fault strands exposed in the trenches are related to either surface fault creep or large coseismic ruptures. Similarly, our recent alignment-array survey and trenching along the central Calaveras at Furtado Ranch (near San Felipe Lake) provides evidence for creep deformation but lacks conclusive evidence for surface fault rupture (Kelson et al., 2003). Thus, at the present time, the question of whether or not the central Calaveras fault may produce large surface-rupturing earthquakes remains unresolved.

### 3.0 FAULT-RELATED GEOMORPHOLOGY OF HALLS VALLEY SITE

---

The Halls Valley site is located along the central Calaveras fault in Joseph D. Grant County Park, approximately 10 km east of the Santa Clara valley near San Jose, California (Figure 1). In the northwestern part of Halls Valley, several possible fault-related lineaments interpreted by Witter et al. (2003) as active traces of the Calaveras fault parallel Arroyo Aguague in the vicinity of Grant Lake, a small water supply reservoir (Figure 4). Approximately 0.5 km northwest of Grant Lake, a north-trending zone of secondary faults exhibits distinctive fault-related geomorphology, including two vernal pools within a north-trending, linear depression defined by tonal and vegetation lineaments on the east and a prominent east-facing scarp on the west (Figure 5).

The prominent linear trough that defines the zone of secondary faults is bound by a 1.5- to 2-m-high east-facing scarp on the west and a distinct vegetation lineament and series of ground water seeps on the east (Figures 6A and 6B). The trough is about 500-m long, 30- to 60-m wide and tapers to the north. Two small ephemeral ponds seasonally occupy the closed depression. The depression presently receives colluvial sediment from the east-facing scarp bordering the western margin of the linear trough. Fine-grained lacustrine (pond) sediment fills the central and southern parts of the depression, and during the wettest years may be deposited across the entire length of the trough. During the dry season when ground water is low, the ponds recede and much of the depression is covered with grasses and marsh vegetation.

#### 4.0 EVIDENCE OF ASEISMIC CREEP AT HALLS VALLEY

---

A small aperture geodetic network crosses the central Calaveras fault zone at the northwestern end of Halls Valley (Figure 5) and provides data to assess rates of aseismic creep and the magnitude of preseismic, coseismic and post-seismic slip following the 1984 Morgan Hill earthquake (Prescott et al., 1984). One of the network stations (shown as “Barn” on Figure 5) is located at the Washburn Barn, approximately 250 m southwest of the Halls Valley trench site (Figure 6A). Periodic line-length measurements between 1977 and two weeks prior to the Morgan Hill earthquake on April 24, 1984 indicate an average right-lateral creep rate across the network of  $9.4 \pm 0.4$  mm/yr. Approximately 70 percent of this slip occurred on a fault strand along the northeastern side of the valley; 30 percent occurred on a strand along the southwestern side of the valley (Prescott et al., 1984). However, we note that the geometry of the network does not indicate whether some of this slip occurred on the secondary faults investigated by this study immediately east of station “Barn”. In contrast to the observations of aseismic slip, no measurable preseismic slip was observed during a survey two weeks prior to the 1984 earthquake. Observations of coseismic changes in the network were consistent with no more than 8.5 mm of right-lateral slip on a fault along the southwestern side of Halls Valley (Prescott et al., 1984). No coseismic slip occurred at the surface along the northeastern margin of the valley and observations after the earthquake indicated no detectible post-seismic slip on either structure. Observations of possible coseismic slip in Halls Valley are contrary to several observations: (1) the Grant Ranch network is located about 5 km northwest of the 1984 epicenter and the northwestern limit of the aftershock zone; (2) fault rupture propagated toward the southeast away from Halls Valley; and (3) no evidence for surface fault rupture was observed during post-earthquake surveys in Halls Valley (Harms et al., 1984) or elsewhere along the inferred length of fault rupture. These observations led Prescott et al. (1984) to question the evidence for coseismic changes from the 1984 earthquake.

Two cultural features that cross the zone of secondary faulting at the Halls Valley site are not deformed and suggest that the secondary faults do not accommodate aseismic creep. The first feature, an old pasture fence, crosses the closed depression normal to the fault zone and bisects the northern tip of the larger of two vernal pools (Figures 6A and 6B). During field reconnaissance, we investigated this fence for evidence of fault creep (e.g., right-laterally offset fence line) and found none. The second feature, Mt. Hamilton Road, obliquely crosses the southern end of the geomorphic trough approximately 500 m south of the trench site (Figure 6A). Our observations along Mt. Hamilton Road for several hundred meters on either side of the projected lineament indicated no signs of buckling, left-stepping en echelon cracking, distortion of pavement, or right-laterally offset curbs or painted road lines. Similarly, we found no evidence for vertical separation across these cultural features consistent with aseismic creep on a fault accommodating dip-slip motion.

## 5.0 SUBSURFACE TRENCHING INVESTIGATION OF SECONDARY FAULT

---

### 5.1 Approach and Methods

Our approach was to investigate the secondary faults and surficial deposits within the linear trough at Halls Valley to assess the timing, style, and sense of recent deformation. The approach also focused on geologic criteria that could be used to evaluate whether or not the secondary fault shows evidence for past creep or coseismic surface rupture. Because there is evidence for the absence of historical creep on the secondary faults that characterize the linear trough, we reasoned that if geologic and geomorphic evidence for surface deformation exists at the site, then it may be a result of past coseismic surface rupture. The results of our trenching investigation are presented in the following sections.

In October 2003, we excavated a 56-m-long trench across the eastern margin and floor of the north-trending linear trough at Grant County Park, to investigate the slip history of the fault and possible evidence for surface fault rupture (Figures 7A and 7B). The exploratory trench was located directly north of a local drainage divide to prevent potential sediment transport into a nearby vernal pool along the fault to the south (Figure 8A). The western extent of the trench was limited by the location of a County Park access road. Stratigraphic and structural relations of the primary fault zone were documented by ~1:20-scale logs of both trench walls. The entire trench was logged at an approximate scale of 1:40. A topographic survey of the immediate area around the trench was completed using an electronic theodolite (Figure 8B). After USGS scientists, local consultants, CGS personnel and other interested parties reviewed the exposures, we backfilled the trench, restored the site to original grade, and reseeded the entire area with native grass seed provided by the Park.

### 5.2 Estimates of Deposit Age

In the absence of suitable material (e.g., charcoal) for radiocarbon dating, the characteristics of prominent argillic soil horizons developed in deeply weathered bedrock (saprolite) and alluvial/colluvial sediments provide qualitative relative age estimates for the deposits encountered in the trench. The soil structure and color, particularly hues of 7.5YR on the Munsell color chart, and thick accumulations of secondary clay evident in the soils suggest long periods of landscape stability at the site. We infer that prominent, thick argillic soil horizons with 7.5 YR hues require several thousand to tens of thousands of years to develop. However, no formal, detailed soil descriptions and/or laboratory analyses that reliably document the characteristics of colluvial soils and their rates of profile development in the eastern San Francisco Bay region have been documented. Therefore, in lieu of radiometric ages, broad estimates of deposit ages relative to adjacent deposits in the exposure are inferred from the interpretation of soil profile development described below.

### 5.3 Near-Surface Stratigraphy

Quaternary deposits encountered in the trench include late Pleistocene to Holocene colluvium and alluvium overlying, or juxtaposed by reverse faults against, rocks of the Franciscan Formation. Stratigraphic relationships in the trench suggest that the depositional environment at the site shifted from an alluvial swale, evident by a buried bedrock strath surface and paleochannel filled with gravel and sand, to the subdued colluvial trough now present at the site. Both environments sustained relatively low rates of deposition based on the limited (<1 to 3 m) total thickness of late Quaternary deposits overlying bedrock at the site. We used soil characteristics such as color and accumulation of secondary clay in argillic soil horizons to qualitatively assess the relative age of surficial deposits exposed in the trench. The absence of detrital charcoal in the deposits prevented quantitative age estimation for the deposits by radiocarbon dating. This section describes the general lithologic characteristics and stratigraphic

relationships between the local bedrock and overlying Quaternary sedimentary packages based on detailed logs of trench exposures (Figures 9, 10 and 11). Detailed descriptions of the geologic units are shown on Figure 9.

Bedrock at the site (unit 1) consists of blocks of fractured sandstone and intensely sheared siltstone within the Late Jurassic to Early Cretaceous Franciscan Formation *mélange* complex (Cotton, 1972). Weathered, indistinctly bedded metagraywacke-type sandstone occurs in the eastern part of the trench (unit 1a). Unit 1b includes massive but indistinct beds of sandstone observed within unit 1a. To the west, a fault-bound block of pervasively sheared *mélange* (unit 1c) consists of dark grey siltstone with vertically oriented quartz veins and clasts of metagreenstone, and exhibits an east-dipping to vertically oriented shear fabric. Two Quaternary active reverse faults, the eastern and western fault strands identified on Figure 9, define the margins of this *mélange* block.

Along the contact between bedrock and overlying colluvium, unit 1a has been altered to a saprolite by pedogenic processes. Units 1dCr and 1eBCr represent residual soil horizons developed in unit 1a (Figure 9). The reddish hue (7.5 YR) and prominent prismatic structure apparent in the upper horizon of this buried soil (unit 1eBCr) suggest that low rates of deposition and landscape stability persisted for a long period of time, perhaps tens of thousands of years, and allowed deep weathering of bedrock exposed near the surface. Following this reasoning, we infer a late Pleistocene age for the bedrock soil. If a coeval soil with similar characteristics was present in unit 1c, then it has been stripped away by erosion because we did not observe prominent soil horizons in the sheared *mélange* (unit 1c) similar to unit 1eBCr (Figure 9). However, moderate prismatic soil structure locally occurs in *mélange* units where hanging-wall uplift caused by slip on the eastern and western fault strands exposed bedrock to surficial weathering (unit 1fCr, Figures 9, 10 and 11). Unit 1fCr represents more recent soil development in hanging-wall bedrock that occurred after tectonic uplift likely caused erosion of the older bedrock soil (units 1dCr and 1eBCr) present in the eastern part of the trench.

Alluvial deposits that fill a buried paleochannel (unit 2) consist of sandy gravel (unit 2a) and gravelly to silty sand (unit 2b). On the eastern side of the paleochannel, the lenticular deposits lap onto a buried bedrock high. On the western side of the paleochannel, the base of unit 2 has approximately 1 m of vertical separation across the eastern fault strand. Unit 2cBt represents an argillic soil horizon developed into unit 2b. Like the possible correlative soil in bedrock to the east (units 1eBCr and 1dCr), the reddish hue (7.5YR) of the soil developed in unit 2b suggests that the deposit is relatively old, perhaps latest Pleistocene in age, but probably not as old as the prominent soil developed in bedrock to the east (units 1cBCr and 1dCr). Assuming the channel deposits and associated soil were deposited horizontally, the entire sedimentary package that occupies the paleochannel appears to be gently tilted to the east by reverse displacement along the eastern fault strand.

In the western part of the trench, colluvial deposits of unit 3 on the west are faulted against intensely-sheared Franciscan *mélange* rocks (unit 1c) on the east. This relatively thick (>1.5 m) sedimentary package consists of gravelly, silty sand (unit 3a) with conspicuous subangular quartz and siltstone clasts derived from *mélange* rocks to the west. Moderate accumulation of secondary clay through pedogenic processes is represented by units 3b and 3cBt. Although clay films lining pores and ped faces in unit 3cBt are prominent, their 10YR hue suggests that the deposits of unit 3 are younger relative to the redder soil profile developed in the paleochannel deposits (unit 2cBt). However, because the laterally adjacent deposits of units 2 and 3 do not overlap, and because both deposits are unconformably overlain by unit 5a, we infer that soil development in unit 2cBt largely predated and continued during the time of soil development in unit 3cBt. On the basis of the moderate soil development observed in unit 3cBt, we estimate a latest Pleistocene to early Holocene age for the deposits mapped as unit 3.

Unit 4 drapes the buried west-facing scarp associated with the eastern fault strand and may represent proximal scarp-derived colluvium (Figures 9, 10 and 11). A concentration of large, subangular clasts of quartz, siltstone and sandstone differentiates this deposit from the overlying unit 5a. The nearest source that contains clasts of this size and composition is gravel in unit 2a that occurs in the hanging wall of the eastern fault strand (Figure 11). Based on the presence of gravel in the hanging wall and on the wedge-like shape of the deposit, we interpret that unit 4 formed by erosion and degradation of a fault scarp produced by surface rupture of the eastern fault strand. We develop this hypothesis further in Sections 5.4.1 and 6.1 below.

A thin (<1-m-thick) package of probable Holocene colluvium (unit 5) mantles the entire site. Subunits within the package consist of light yellowish brown sandy silt (unit 5a) and pale yellow silty sand (unit 5b) (Figure 9). Pedogenic development in the deposit includes Bw- and A-soil horizons, depicted as units 5cBw and 5dA, respectively.

## **5.4 Near-Surface Structural Relationships**

The Halls Valley trench exposed two northwest-striking, east-dipping reverse faults that displace latest Pleistocene to Holocene alluvium and colluvium deposited in a north-trending linear trough (Figure 8). The eastern fault strand offsets the western margin of a paleochannel and caused gentle eastward tilting of lenticular beds and a soil developed in the channel deposits (Figures 9 and 10). The western fault strand places Franciscan mélangé rocks over probable latest Pleistocene to early Holocene colluvium (Figure 11). Neither fault strand reaches the ground surface nor disrupts youngest probable middle to late Holocene colluvial sediment (units 4 and 5; Figure 9). Although we find it unlikely, it is possible that a third fault exists along the western margin of the valley beneath an access road that prevented further excavation to the west. The thickness of the colluvial deposits of unit 3, bedrock deeper than 2 m and inferred fault-related lineaments west of the excavation, suggest the possibility that a third fault may exist west of the trench along the east-facing valley margin. The following section presents brief descriptions of the eastern and western fault strands observed in the trench.

### **5.4.1 Eastern Fault Strand**

The eastern fault strand consists of a narrow shear zone, 0.01 to 0.20 m wide at the base of the trench, that divides upward into multiple fault splays where the fault cuts alluvial deposits of unit 2 (Figures 9 and 11). The fault zone reaches a maximum width of 0.5 to 1 m where several fault splays terminate below units 4 and 5. The most prominent shears along the fault strike  $335^{\circ}$  to  $347^{\circ}$  and dip  $56^{\circ}$  NE (see note b, Figure 10 and note a, Figure 11). The eastern fault strand offsets Franciscan mélangé (units 1b and 1c) and alluvial deposits (units 2a and 2b) along the western margin of the paleochannel. Displacement of bedrock in the hanging wall over unit 2a in the footwall indicates a component of reverse slip. Total vertical displacement of the base of unit 2a is at least 1 m. Assuming pure dip-slip displacement as indicated by slickenside striations on the fault plane (Figure 12), the total offset of the base of unit 2a along the fault plane is approximately 1.2 m and probably reached about 1.5 m if the slip estimate accounts for a moderate amount of scarp degradation.

Possible evidence for surface fault rupture on the eastern fault strand includes an inferred scarp-derived colluvial wedge (unit 4), and multiple fault strands that terminate in the hanging-wall scarp buried by units 4 and 5. Scarp-derived colluvial wedges produced by reverse faulting consist of a proximal facies that includes large blocks of soil and strata resulting from collapse of the hanging wall, and a distal facies that consists of fine-grained material transported by surficial processes that record the gradual decline of the scarp (Carver and McCalpin, 1996). Although unit 4 lacks obvious large hanging wall blocks typical of proximal colluvial deposits, it consists of a wedge-shaped concentration of subangular gravel clasts derived from unit 2a that tapers away from the scarp—satisfying criteria consistent with decline of fault

scarps produced by surface rupture (Weber and Cotton, 1980). Degradation and beveling of the fault scarp also is evident by the truncation of paleochannel deposits along the angular unconformity at the base of unit 5a. Indirect evidence for coseismic surface rupture is shown by signs of extensive past erosion at the site (discussed above) including a bedrock strath underlying unit 2a east of the fault, and an unconformity at the base of unit 5 in addition to degradation of the buried fault scarp evident by scarp-derived colluvium. Such strong indications of erosion implies that the scarp is related to surface rupture and not a vertical component of aseismic creep because at this site erosion rates would out pace gradual scarp growth via creep. Although, aseismic creep that includes a vertical component of slip is a viable mechanism to produce fault scarps, we favor coseismic surface rupture as the best explanation for fault-scarp formation and subsequent deposition of unit 4 based on the reasoning presented above and developed further below in Section 6.1.

If unit 4 was derived from a scarp produced by surface fault rupture, then it records scarp decline following the most recent earthquake on this fault because several subvertical and steeply east-dipping fault splays terminate below the unconformity that marks the base of units 4 and 5. Evidence for scarp-derived colluvium produced by earlier surface rupturing earthquakes is equivocal. For instance, exposures on both trench walls show triangular-shaped deposits interpreted as unit 2a directly above the fault tip (Figures 10 and 11). This feature may be interpreted in one of two ways: (1) a scarp-derived colluvial wedge formed after the penultimate earthquake ground rupture; or (2) sediment from unit 2a that has been “bulldozed” or pushed up in front of the leading edge of the hanging wall block. Alternatively, considering the evidence for erosive processes that cut the strath surface in unit 1c, colluvial wedges formed from earlier scarp-producing events may not have been preserved. In support of this possibility, Weber and Cotton (1980) concluded that surface displacements less than 0.3 to 0.5 m may not produce a distinct colluvial wedge recognizable in trench exposures.

We interpret that multiple surface rupturing earthquakes have occurred on the eastern fault strand based on progressively greater amounts of deformation of soils and strata of increasing age. Evidence for at least two surface displacement events are suggested by: (1) reverse offset of a buried soil developed in bedrock (unit 1fCr) and surficial deposits (units 2cBt and 3cBt) that has a vertical component of about one third (~0.3 m) of the vertical component of offset of the base of unit 2a; and (2) progressively greater tilting of the paleochannel deposits (unit 2) with depth (and increasing age). Reverse offset of a buried soil developed in the hanging wall scarp and footwall of the eastern fault strand (Figures 10 and 11) reflects displacement during the most recent event. In the footwall, this soil is developed surficial deposits (units 2a and 3cBt) and, to a lesser extent, in bedrock (unit 1fCr) overlain by a thin gravel lag deposit of unit 2a that tapers to the west. To the east near the fault, where the hanging wall overrides the footwall, the gravel deposit of unit 2a thickens dramatically and there is no soil developed in unit 2a or the underlying bedrock. This observation indicates that the soil formed after erosion beveled the bedrock strath and deposition of unit 3cBt. The same soil (unit 1fCr) also is developed in bedrock in the hanging wall and in the youngest deposits within the buried channel (unit 2cBt). Formation of the soil in the hanging wall must have occurred after initial fault displacement exposed bedrock at the surface because no soil development is evident within or below the thickest channel deposits of unit 2a in the footwall. The estimated vertical component of displacement of the most recent surface rupture is 0.3 to 0.5 m based on direct measurement of the top of the soil offset across the fault (Figures 10 and 11). In contrast, the base of unit 2a is vertically displaced by at least 1 m (Figure 11). Such evidence for progressive displacement of strata with depth, coupled with suggestive evidence for surface fault rupture, implies that the trench exposures record multiple earthquakes.

Notably, there is an absence of evidence for historical creep in deposits that directly overlie the eastern fault strand. All fault strands terminate below units 4 or 5a; no fractures or shear zones continue to the surface as observed on actively creeping strands of the central Calaveras fault (e.g., Kelson et al., 2003).

#### 5.4.2 Western Fault Strand

The western fault strand includes both a primary, northwest-striking, east-dipping reverse fault and a secondary north-to-northeast-striking, west-dipping backthrust. The primary reverse fault places sheared Franciscan mélangé over early Holocene (?) colluvium of unit 3 (Figure 11). Striations in slickensides indicate pure dip-slip motion on the primary fault plane that strikes  $347^{\circ}$  and dips  $56^{\circ}$ NE (Figure 11). An undulatory fault plane characterizes a west-dipping fault splay that varies in strike from  $003^{\circ}$  to  $020^{\circ}$  and dips  $60^{\circ}$  to  $87^{\circ}$  W. Striations in slickensides have rakes of about  $70^{\circ}$  (measured clockwise from strike) and indicate predominantly reverse displacement with a minor oblique component of right-lateral slip. We interpret this fault splay as a backthrust above the primary reverse fault. The backthrust splays off of the primary fault in unit 3a and cuts upsection into unit 3cBt but terminates about 0.3 m below the base of unit 5b.

Details of the displacement history on the western fault strand are difficult to interpret because of an absence of evidence for surface fault rupture and deep weathering in the soil profile of unit 3cBt near the secondary backthrust (Figure 11). The notable absence of proximal scarp-derived colluvial wedges, collapsed hanging-wall material, sediment-filled fissures and multiple upward fault terminations—criteria indicative of surface fault rupture (e.g., Nelson, 1992; Weldon et al., 1996)—leaves open the possibility that slip on the western strand occurred predominantly through aseismic creep. However, undeformed deposits of unit 5 that overlie the fault preclude the possibility of recent or ongoing creep.

## 6.0 DISCUSSION

---

### 6.1 Possible Evidence for Surface Fault Rupture and Implications for Seismic Hazard

Several lines of evidence support the interpretation that the eastern strand within the zone of secondary faults ruptured the surface in latest Pleistocene to early Holocene time. First, unit 4 is a wedge-shaped deposit of colluvium that tapers westward, away from a buried fault scarp and contains coarse gravel clasts most likely derived from unit 2a in the hanging wall. We interpret unit 4 as the proximal colluvial facies produced by degradation and erosion of a fault scarp produced by surface rupture. Second, multiple fault strands terminate below the unconformity at the base of units 4 and 5a. The observation that the fault strands do not reach the surface or deform overlying deposits defines an event horizon and provides corroborative evidence for surface fault rupture. Finally, the presence of a buried fault scarp directly adjacent to a beveled strath surface cut into Franciscan bedrock indicates that the rate of scarp growth was greater than the rate of erosion at the time of deformation. Both the basal unconformity of unit 5a and the buried bedrock strath surface indicate that erosion processes dominated at the site before and after deformation that produced the fault scarp. Based on this evidence, we infer that slow, vertical scarp growth by aseismic creep at rates less than 9 mm/yr (Prescott et al., 1984) would be outpaced by erosion. More likely, the scarp was produced instantaneously by coseismic surface fault rupture and became buried by unit 5a before it was entirely degraded by erosion.

Do stratigraphic and structural relations in the trench refute the hypothesis that the central Calaveras fault releases strain solely through aseismic creep and moderate ( $M \leq 6.2$ ) magnitude earthquakes? If the hypothesis is true, then the geomorphic expression of secondary faults oriented at high angles to the principal direction of right-lateral shear strain (approximately N 30° W) should be a product of slow creep or after-slip following Morgan Hill-type events. Such faults should be expressed in trench exposures as anastomosing strands that reach the ground surface. Furthermore, these fault strands should not terminate below a common stratigraphic layer, and should not be associated with unconformity bounded scarp-derived colluvial packages or sediment filled fissures. The trench exposures documented by this study show provocative features that satisfy two of these three criteria: the eastern fault strand is overlain by an interpreted scarp-derived colluvial wedge and fault strands terminate below the youngest colluvial deposits (units 4 and 5a). In addition, field surveys show that historical cultural features that cross the north-trending Halls Valley lineament are not deformed and trench exposures lack fault strands that reach the surface suggesting that these secondary faults do not creep or, if they have released strain via creep in the past, they are not creeping now. The timing of deformation on the secondary faults is poorly constrained due to the lack of dateable carbon in the trench. However, we interpret at least one event in the Holocene based on a notable lack of soil development in deposits (units 4 and 5) that overlie the buried fault scarp. Although the evidence is not definitive and may be subject to alternative interpretations, the results of this investigation leave open the possibility that the central Calaveras fault is capable of producing surface fault rupture.

Possible evidence for surface fault rupture on secondary strands of the central Calaveras fault has implications to earthquake hazard estimates in the southern San Francisco Bay area. Current probabilistic hazard assessments assign a low weight to rupture scenarios that involve large ( $M \geq 6.2$ ) earthquakes on the central Calaveras fault. Although the evidence is not definitive, geologic data (e.g., Baldwin et al., 2002; Kelson et al., 1998) can be interpreted as evidence for coseismic surface fault rupture and may build a case for fault rupture scenarios that involve large-magnitude ( $M \geq 6.2$ ) earthquakes along the central Calaveras fault. This investigation highlights the need to conduct further paleoseismic studies to better characterize the seismic potential of the central Calaveras fault and further test the hypothesis that the fault is not capable of generating large-magnitude earthquakes.

## 6.2 Slip History of Secondary Faults in Halls Valley

Observations from the trench exposures provide evidence for at least two and possibly three episodes of reverse displacement on secondary faults at the Halls Valley site. The most recent earthquake likely produced reverse displacement that offset a moderate soil developed in alluvium and bedrock exposed in the hanging wall (units 2cBt and 1fCr, Figures 10 and 11), and a correlative soil developed in thin colluvial deposits and underlying bedrock in the footwall (units 3cBt and 1fCr). Vertical separation of the soil is at least 0.3 m and possibly as much as 0.5 m if scarp erosion is taken into account. Degradation of the scarp resulted in the deposition of a proximal colluvial wedge (unit 4). Striated slickensides on the fault plane indicate pure dip-slip movement and repeated strata across the fault indicate reverse displacement. Total displacement on the fault plane, calculated by trigonometric relations given 0.3 to 0.5 m vertical separation, a  $56^\circ$  dip and pure dip-slip motion, ranges from 0.4 to 0.6 m.

Evidence for at least one additional earthquake comes from progressively greater offset and gentle eastward tilting of paleochannel deposits in the hanging wall (unit 2a, 2b, and 2cBt) with depth. The total estimated displacement of the base of the paleochannel in the hanging wall (unit 2a), assuming pure reverse motion, ranges from 1.2 to 1.5 m. As discussed above, the estimated displacement of the base of unit 2a is about three times the estimated displacement of unit 1fCr produced by the most recent earthquake. In addition, we conclude that the most recent event ruptured the surface as indicated by a proximal scarp-derived colluvial wedge (unit 4). If our interpretations are correct and two earthquakes are recorded in the trench exposures, then the total reverse displacement for the penultimate event ranged from 0.6 to 1.1 m. However, if the amount of slip during prior events equaled the estimated slip during the most recent event (0.4 to 0.6 m), then stratigraphic and structural relationships in the trench may record three earthquakes.

The slip history of the western fault strand differs from that of the eastern fault strand. The youngest deposit offset by the western strand (unit 3cBt, Figure 11), does not extend across the eastern strand and, therefore, is not offset by it. However, unit 3cBt is overlain by unit 4, a deposit that we interpret is a proximal scarp-derived colluvial wedge formed after the most recent event on the eastern strand. These stratigraphic relations suggest that the most recent displacement on both the eastern and western strands occurred after deposition of unit 3cBt but prior to deposition of unit 4. The exposures lacked any geologic data that would require coseismic slip on both faults simultaneously. Furthermore, the absence of geologic evidence for surface fault rupture on the western strand allows the possibility that it predominantly released strain by aseismic creep, but no evidence was observed that precludes coseismic fault rupture. If fault creep did occur it probably has since stopped because none of the fault splays reach the surface and colluvial deposits of unit 5 that overlie the western strand are undeformed.

A third fault strand, not crossed by the trench excavation, may exist along the western margin of the Halls Valley site. Several possible fault-related, north- to northwest-trending vegetation and tonal lineaments, interpreted on aerial photographs (Figure 5) and identified in the field (Figure 6A) occur along the margins and obliquely cross the valley south of the trench. One particularly prominent lineament bounds the western sides of two vernal pools and projects northward along the western valley margin under an access road west of the trench (Figure 6A). Anomalously thick colluvial deposits (>2 m) in the western end of the trench (Figure 11) also suggest the presence of a fault along the western margin of the linear valley. If a third fault does exist west of the trench, then our results do not characterize the entire zone of secondary deformation at the Halls Valley site.

## 6.3 Possible Explanations for Reverse Faults in Halls Valley

The orientation and style of faulting evident in the trench exposure is contrary to our regional kinematic model developed from surficial geologic and geomorphic mapping of the central Calaveras fault (Witter

et al., 2003), from which we would expect right-stepping transtensional deformation. We propose two possible explanations for the fault geometry and slip direction shown in the trench that likely reflect local stress perturbations along the fault. First, secondary reverse faults that bound pop-up structures near the ends of pull-apart basins have been observed in analog models and natural examples of releasing stepovers along strike slip faults (e.g., Dooley and McClay, 1997). The structural style of the reverse faults documented at Halls Valley, their location, and the hill to the east of the faults that may reflect a local pop-up structure, are similar to the simulated geometry and style of faulting observed for analog models of pull-apart basins (Figure 13). Alternatively, contractional deformation west of the central Calaveras fault may reflect the westward transfer of slip onto the southern Hayward fault.

The general distribution of faults, fault styles and the geometry of the pull-apart basin at Halls Valley share many similarities to fault maps of pull-apart basins interpreted from analog sandbox models (Figure 13). Dooley and McClay (1997) performed several experiments using scaled sandbox models designed to simulate the kinematic evolution of pull-apart basins above releasing stepovers in right-lateral fault systems. Their models illustrate the progressive evolution of pull-apart basins by simulating various releasing geometries in the basement fault system including underlapping, overlapping and right angle stepover configurations. During the initial stages of the experiments, Riedel shears originate above the stepover in the basement fault. As displacement increases, additional Riedel shears develop above the main underlying fault strands away from the stepover, and are termed the principal displacement zones. Broad uplifted blocks bound by oblique reverse faults, termed borderland structures, flank the principal displacement zone, near the ends of the evolving basin. With further displacement, the borderland structures become inactive. Development of the pull-apart structure is accommodated by increasing right-lateral separation of the principal displacement zones that form the sidewalls of the basin. Eventually, as the basin grows, oblique extensional faults form terraced sidewalls and a through-going, anastomosing zone of right-lateral faults develops across the floor of the basin.

The pop-up structures associated with oblique reverse faults observed in the sand box experiments of Dooley and McClay (1997) provide an analog case for the secondary reverse faults investigated at the Halls Valley site. Observations from analog models and Halls Valley reveal oblique reverse and pure reverse (in the case of Halls Valley) faults that bound local uplifted blocks near the apices of rhomb-shaped basins formed by releasing fault stepovers (Figure 13). The pop-up structures formed shortly after displacement was initiated during the sandbox experiments. This observation suggests that the reverse faults we investigated may have formed during the initial development of the pull-apart basin at Halls Valley.

An alternative explanation for reverse faults at the northwestern end of Halls Valley is that they may accommodate contraction caused by the transfer of slip between the central Calaveras and southern Hayward faults. Transpressional deformation in the eastern San Francisco Bay area includes northwest-southeast oriented, en echelon thrust faults and folds typical of a dextral wrench tectonic setting (Unruh and Lettis, 1998). However, contractional structures in the East Bay region are oriented about 40° more westerly than the north-northwest strikes of the reverse faults encountered at Halls Valley. Although these reverse faults clearly are not compatible with the regional strain field dominated by north-south directed principal strain (Unruh and Lettis, 1998), they may reflect a local aberration in the strain field. The geologic data collected at Halls Valley do not elucidate whether these reverse faults are related to the development of the Halls Valley pull-apart basin or to complex strain patterns related to the westward transfer of slip onto the southern Hayward fault.

## 7.0 SUMMARY OF FINDINGS

---

The results of this investigation show evidence for reverse displacement on two faults that strike N 20° to 40° W and dip 47° to 56° NE. Both faults cut probable late Pleistocene to early Holocene colluvial and alluvial deposits that locally mantle Franciscan greywacke and mélangé. Slickensides on the fault planes indicate pure dip-slip movement and the sense of vertical separation of strata indicates reverse displacement. The estimated total amount of dip-slip displacement based on measurements of the reverse offset of the base of a late Pleistocene alluvial channel ranges from 1.2 to 1.5 m.

Possible evidence for surface rupture includes a proximal colluvial wedge (unit 4) derived from erosion of alluvial gravel in the hanging wall and multiple fault strands that terminate beneath colluvium that buries the scarp along an unconformity. In addition, evidence for high rates of erosion before and after surface fault rupture favors the interpretation that scarp construction was caused by surface rupture because high surface erosion rates would likely outpace the much slower rate of scarp growth produced by a vertical component of aseismic creep. We interpret that scarp formation occurred during the most recent event that displaced a prominent buried soil by 0.4 to 0.6 m. Because we interpret the colluvial wedge (unit 4) to be early to middle Holocene in age, we infer a similar age for the time of the most recent deformation event.

Increasing amounts of reverse displacement and eastward tilting of alluvial strata in the buried channel with depth indicate that multiple earthquakes may have ruptured the surface. Although evidence of a scarp-derived colluvial wedge and upward terminating fault strands satisfy criteria for surface fault rupture during the most recent event, stratigraphic evidence for earlier episodes of deformation lacked these diagnostic features and provides no information to assess whether fault movement involved surface rupture or creep. By comparing the total estimated dip-slip displacement of the base of the alluvial channel (1.2 to 1.5 m) to the estimated displacement of a soil developed in units 2cBt, 3cBt and 1fCr, we interpret that the trench exposures record at least two and possibly three earthquakes that produced 0.4 to 1.1 m slip per event. The youngest colluvial deposits showed no evidence of displacement or deformation above the fault, suggesting that this fault has not experienced aseismic creep since the most recent earthquake. There is no evidence within the trench that can conclusively be attributed to aseismic fault creep.

We did not expect to encounter reverse faulting at the northwestern end of Halls Valley along a section of the central Calaveras fault zone previously interpreted as a 1- to 1.5-km-wide extensional stepover (Witter et al., 2003). Two possible explanations for the secondary reverse faults observed at the Halls Valley site include: (1) the observation of secondary reverse faults, termed “borderland structures” that form near the ends of pull-apart basins documented in experimental sandbox models of releasing stepovers along strike slip faults (e.g., Dooley and McClay, 1997); and (2) contractional deformation west of the central Calaveras fault related to the westward transfer of slip onto the southern Hayward fault. Because these faults clearly are not compatible with the regional East Bay strain field dominated by north-south directed principal strain (Unruh and Lettis, 1998), they likely reflect local strain field aberrations due to complex fault interactions. The geologic data collected at the Halls Valley site do not distinguish the validity of either explanation.

If the trench exposures documented by this investigation hold evidence for surface fault rupture, our preferred interpretation of the geological data, then seismic hazard assessments should reevaluate the seismic potential of the central Calaveras fault. Surface displacement of up to 1 m is consistent with large ( $M \geq 6.2$ ) earthquakes that likely produced surface fault rupture in excess of 10 km in length. An earthquake of this magnitude likely would severely impact the heavily urbanized Santa Clara valley through strong shaking and liquefaction-related ground deformation. The results of this study, although

not definitive, emphasize the need to conduct further subsurface investigations of active traces of the central Calaveras fault zone that may reflect surface fault rupture.

## **8.0 ACKNOWLEDGMENTS**

---

We thank the Santa Clara County Department of Parks and Recreation for permission to conduct this trenching investigation in Joseph D. Grant County Park. Don Rocha, the Parks Natural Resources Program Supervisor, and John Goldsworthy, the Park Use Coordinator, assisted with the permitting process. Park Rangers Jeff Cossins and Bruce Johnson were particularly helpful in providing access to the site, assisting with mandatory fire mitigation measures, and provided seed and personnel to revegetate the site. Ashley Streig of William Lettis & Associates, Inc. contributed in the field during the project and Carolyn Mosher produced the graphics. Finally, we thank Billy Vaughan of Euro-Tech Construction for his adept and efficient excavation of the trenches and safe navigation along the very windy Mt. Hamilton road that leads to the site. Reid Fisher, Bill Bryant, Kevin Clahan, Bill Lettis, Tom Fumal, David Schwartz, Suzanne Hecker, Jim Lienkaemper and Heidi Stenner participated in the trench review.

## 9.0 REFERENCES

---

- Andrews, D.J., Oppenheimer, D.H., and Lienkaemper, J.J., 1993, The Mission link between the Hayward and Calaveras Faults: *Journal of Geophysical Research*, v. 98, p. 12,083-12,095.
- Aydin, A., and Page, B.M., 1984, Diverse Pliocene-Quaternary tectonics in a transform environment, San Francisco Bay region, California: *Geological Society of America Bulletin*, v. 95, p. 1303-1317.
- Bakun, W.H., 1980, Seismic activity on the southern Calaveras fault in central California: *Bulletin of Seismological Society of America*, v. 70, p. 1181-1197.
- Bakun, W.H., 1984, Seismic moments, local magnitudes, and coda duration magnitudes for earthquakes in central California: *Bulletin of Seismological Society of America*, v. 74, p. 439-458.
- Bakun, W.H. and Lindh, A.G., 1985, Potential for future damaging shocks on the Calaveras fault, California: U.S. Geological Survey Open-File Report 85-754, p. 266-279.
- Bolt, B.A. and Miller, R.D., 1975, Catalogue of earthquakes in northern California and adjoining areas, *in* *Seismographic Stations*, University of California Press, Berkeley, p. 7-18.
- Baldwin, J.N., Kelson, K.I., Witter, R.C., Koehler, R.D., Helms, J.G., and Barron, A.D., 2002, Preliminary report on the late Holocene slip rate along the central Calaveras Fault, southern San Francisco Bay area, Gilroy, California: Final Technical Report submitted to the National Earthquake Hazard Reduction Program, 27 p.
- Burford, R.O. and Sharp, R.V., 1982, Slip on the Hayward and Calaveras faults determined from offset powerlines: California Division of Mines and Geology, Special Publication 62, p. 261-269.
- Carver, G.A., and McCalpin, J.P., 1996, Paleoseismology of Compressional Tectonic Environments, *in* McCalpin, J.P., ed. *Paleoseismology*, Academic Press, p. 183-269.
- Cockerham, R.S., and Eaton, J.P., 1987, The earthquake and its aftershocks, April 24 through September 30, 1984, *in* Hoose, S.A., ed., *The Morgan Hill, California, Earthquake of April 24, 1984*: U.S. Geological Survey Bulletin 1639, p. 15-28.
- Dooley and McClay, 1997, Analog modeling of pull-apart basins: *AAPG Bulletin*, v. 81, no. 11, p. 1804-1826.
- Du, Y. and Aydin, A., 1993, Stress transfer during three sequential moderate earthquakes along the central Calaveras Fault, California: *Journal of Geophysical Research*, v. 98, p. 9947-9962.
- Ellsworth W.L., Olsen, J.A., Shijo, L.N., and Marks, S.M., 1982, Seismicity and active faults in the eastern San Francisco Bay region, *in* Hart, E.W., Hirshfeld, S.E. and Schulz, S.S., eds., *Proceedings of the Conference on Earthquake Hazards in the Eastern San Francisco Bay Area*: California Division of Mines and Geology Special Publication 62, p. 83-91.
- Fenton, C.H. and C.S. Hitchcock, 2001, Recent geomorphic and paleoseismic investigations of thrust faults in Santa Clara Valley, California, *in* Ferriz, H. and Anderson, R., eds., *Engineering Geology Practice in Northern California*: Division of Mines and Geology Bulletin 210, Association of Engineering Geologists Special Publication 12, p. 239-257.
- Galehouse, J.S., and Lienkaemper, J.J., 2003, Inferences drawn from two decades of alignment array measurements of creep on faults in the San Francisco Bay Region: *Bulletin of the Seismological Society of America*, v. 93, n. 6, p. 2415-2433.

- Graymer, R., 1995 Geology of the southeast San Francisco Bay area hills, California, *in* Sanginés, E.M., Andersen, D.W., and Busing, A.B., eds., *Recent Geologic Studies in the San Francisco Bay Area: Pacific section S.E.P.M.*, v. 76, p. 115-124.
- Harms, K.K., Clark, M.M., Rymer, M.J., Bonilla, M.G., Harp, E.L., Herd, D.G., Lajoie, K.R., Lienkaemper, J.J., Mathieson, S.A., Perkins, J.A., Wallace, R. E., and Ziony, J.I., 1987, The search for surface faulting, *in* Hoose, S.A., ed., *The Morgan Hill, California, Earthquake of April 24, 1984*: U.S. Geological Survey Bulletin 1639, p. 61-68.
- Kelson, K.I., Baldwin, J.N., and Brankman, C.M., 2003, Late Holocene displacement of the Central Calaveras Fault, Furtado Ranch Site, Gilroy, CA: Final Technical Report submitted to the National Earthquake Hazard Reduction Program, 38 p.
- Kelson, K.I., Baldwin, J.N., and Randolph, C.E., 1998, Late Holocene slip rate and amounts of coseismic rupture along the central Calaveras fault, San Francisco Bay area, California: Final Technical Report submitted to the National Earthquake Hazard Reduction Program, 26 p.
- Kelson, K.I., Lettis, W.R., and Lisowski, M., 1992a, Distribution of geologic slip and creep along faults in the San Francisco Bay Region: California Division of Mines and Geology, Special Publication 113, p. 31-38.
- Kelson, K.I., Simpson, G.D., Lettis, W.R., and Haraden, C., 1996, Holocene slip rate and earthquake recurrence of the northern Calaveras fault at Leyden Creek, northern California: *Journal of Geophysical Research*, v. 101, no. B3, p. 5961-5975.
- Lisowski, M. and King, N., 1982, Geodetic surface slip along the rupture zone of the Coyote Lake, California earthquake, unpublished manuscript, 28 pp.
- Nelson, A.R., 1992, Lithofacies analysis of colluvial sediments - an aid in interpreting the recent history of Quaternary normal faults in the Basin and Range province, western United States: *Journal of Sedimentary Petrology*, v. 62, p. 607-621.
- Oppenheimer, D.H., Bakun, W.H., and Lindh, A.G., 1990, Slip partitioning of the Calaveras fault, CA, and prospects of future earthquakes: *Journal of Geophysical Research*, v. 95, no. B6, p. 8483-8498.
- Prescott, W.H., Lisowski, M., and Savage, J.C., 1981, Geodetic measurement of crustal deformation on the San Andreas, Hayward, and Calaveras faults near San Francisco, California: *Journal of Geophysical Research*, v. 86, p. 10,853-10,869.
- Prescott, W.H. and Lisowski, M., 1983, Strain accumulation along the San Andreas fault system east of San Francisco Bay, California: *Tectonophysics*, v. 97, p. 41-56.
- Prescott, W.H., King, N.E., and Guohua, G., 1984, Preseismic, coseismic and postseismic deformation associated with the 1984 Morgan Hill, California, earthquake: California Division of Mines and Geology, Special Publication 68, p. 137-148.
- Schaff, D.P., Bokelmann, G.H.R., Beroza, G.C., Waldhauser, F. and Ellsworth, W.L., 2002, High-resolution image of Calaveras Fault seismicity: *Journal of Geophysical Research*, v. 107, n. B9, ESE 5, p. 1-16.
- Simpson, G.D., Baldwin, J.N., Kelson, K.I., Lettis, W.R., 1999, Late Holocene slip rate and earthquake history for the northern Calaveras fault at Welch Creek, eastern San Francisco Bay area, California: *Bulletin of Seismological Society of America*, v. 89, p. 1250-1263.
- Stenner, H., Ueta, K., and Hamilton, J.C., 1999, Looking for evidence of large surface ruptures along the southern Calaveras fault [abs.]: *Eos (Transactions, American Geophysical Union)* v. 80, no. 46, p. F735.

- Topozada, T.R., Real, C.R., and Parke, D.L., 1981, Preparation of isoseismal maps and summaries of reported effects for pre-1900 California earthquakes: California Division of Mines and Geology Open File Report 81-11 SAC, 182 pp.
- Topozada, T.R. and Parke, D.L., 1982, Areas damaged by California earthquakes, 1900-1949: California Division of Mines and Geology Open-File Report 82-17 SAC, 65 pp.
- Unruh, J.R. and Lettis, W.R., 1998, Seismogenic deformation field in the Mojave block and implications for tectonics of the eastern California shear zone: *Journal of Geophysical Research*, v. 101, p. 8335-8361.
- Weber, G.E., and Cotton, W.R., 1980, Geologic Investigation and Recurrence Intervals and Recency of Faulting Along the San Gregorio Fault Zone, San Mateo County, California: Unpublished Final Technical Report to the U.S. Geological Survey, contract 14-08-0001-16822. Wm. Cotton & Associates, Los Gatos, CA.
- Weldon, R.J., McCalpin, J.P., and Rockwell, T.K., 1996, Paleoseismology of strike-slip tectonic environments *in*, McCalpin, J.P., ed., *Paleoseismology*, Academic Press, San Diego, p. 271-329.
- Witter, R.C., K.I. Kelson, A.D. Barron, and S.T. Sundermann, 2003, Map of Active Fault Traces, geomorphic features and Quaternary surficial deposits along the central Calaveras fault, Santa Clara County, California: U.S. Geological Survey, National Earthquake Hazards Reduction Program Final Technical Report, Award No. 01HQGR0212, 32 p.
- Wong, I.G. and Hemphill-Haley, M.A., 1992, Seismicity and faulting near the Hayward and Mission Faults, *in* Borchardt, G. et al., eds., *Proceedings of the Second Conference on Earthquake Hazards in the Eastern San Francisco Bay Area*: California Division of Mines and Geology Special Publication 113, p. 207-215.
- Working Group on California Earthquake Probabilities (WGCEP), 2003, Earthquake probabilities in the San Francisco Bay region: 2002-2031: U.S. Geological Survey Open-File Report 03-214.
- Working Group on Northern California Earthquake Potential (WGNCEP), 1996, Database of potential sources for earthquakes larger than magnitude 6 in northern California: U.S. Geological Survey Open-File Report 96-705, 40 p.

## FIGURES

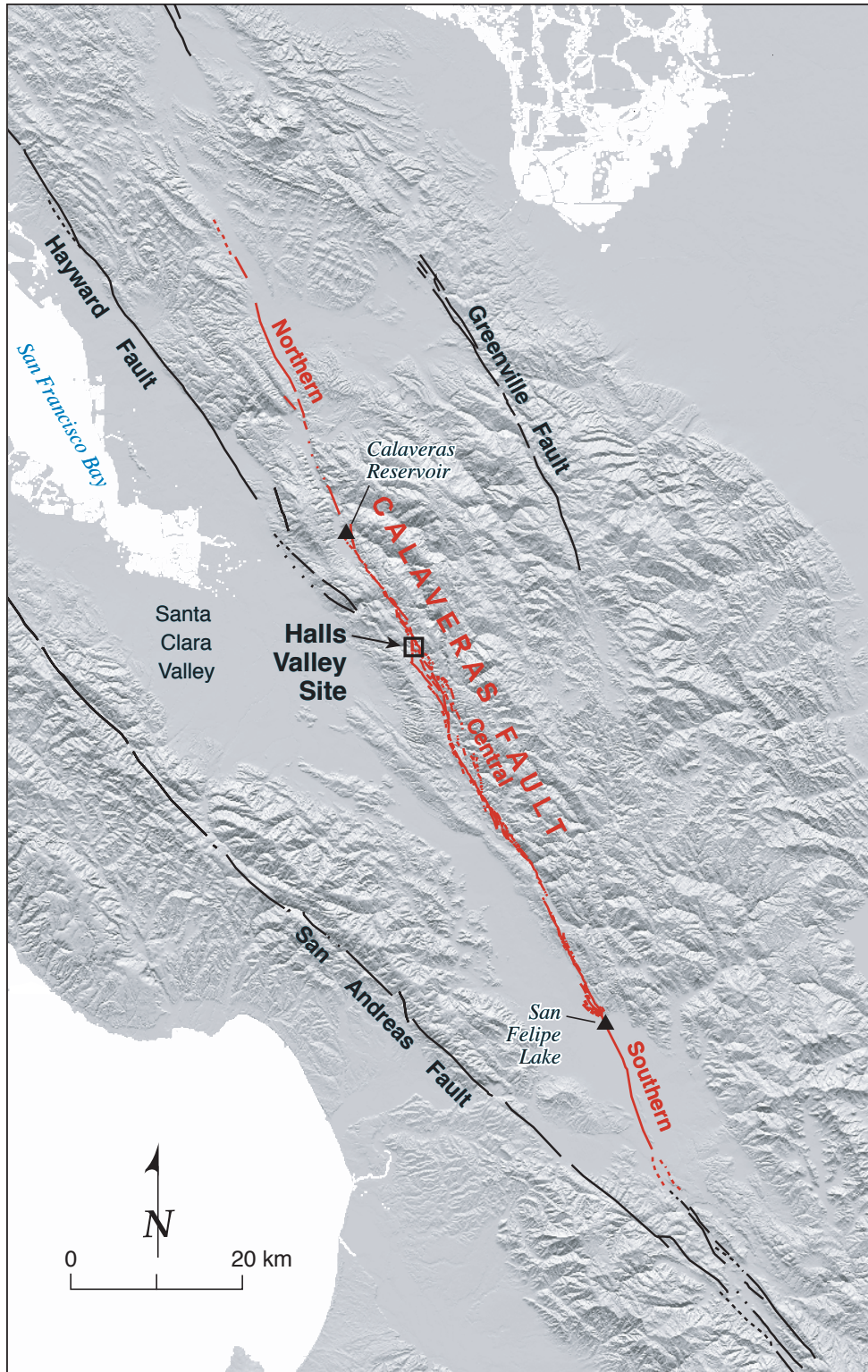


Figure 1. Shaded relief map of the major active faults in the southern San Francisco Bay region. The Halls Valley study site is shown along the central Calaveras fault in Joseph D. Grant County Park. Inferred segment boundaries (shown by ▲ s) near Calaveras Reservoir and San Felipe Lake separate the central Calaveras fault from the adjacent northern and southern sections of the fault.

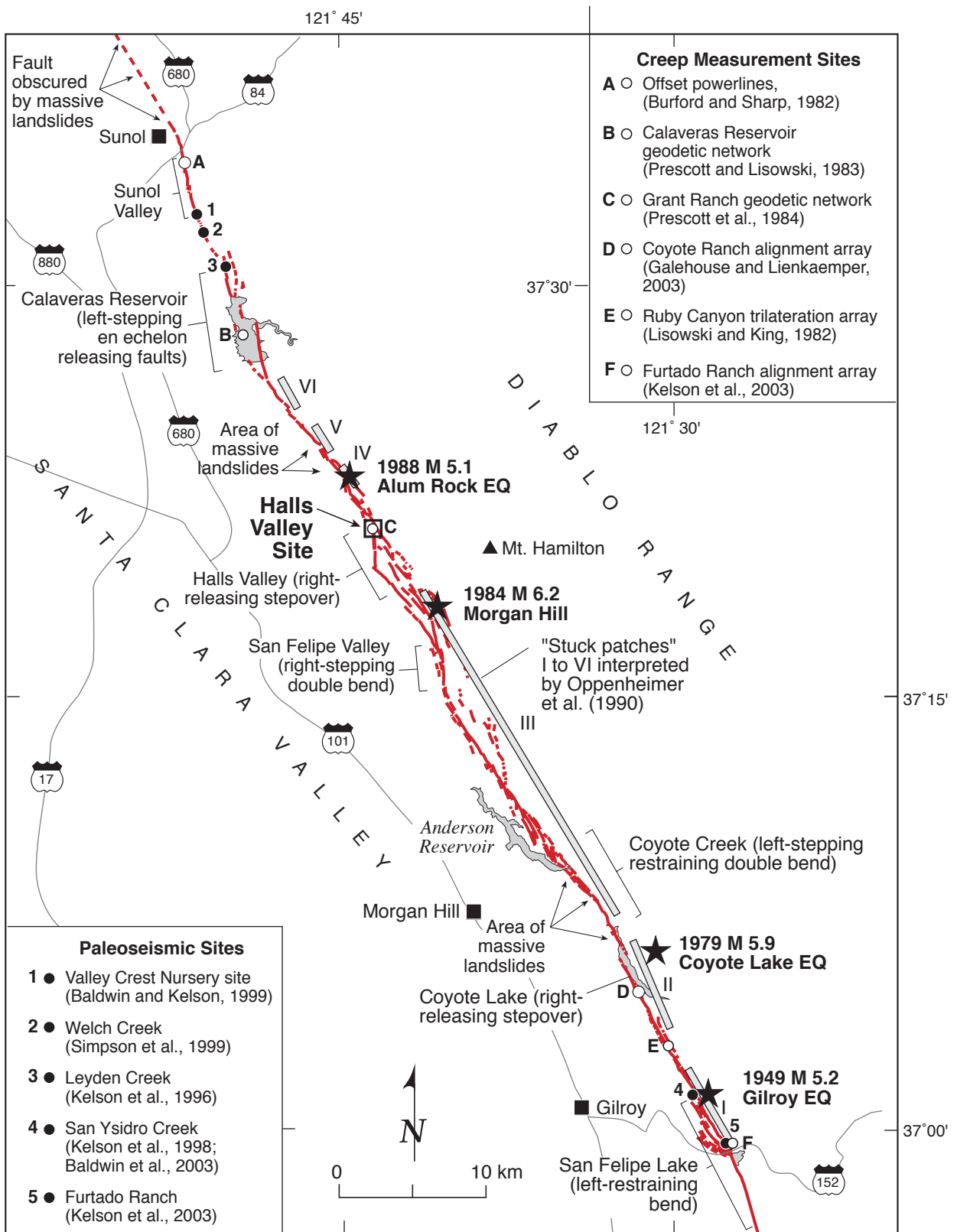


Figure 2. Simplified map of active traces of the central Calaveras fault, showing previous sites of paleoseismic investigation (shown by ●), existing creep measurement sites (shown by ○) and the Halls Valley study site. Historic M >5 earthquake epicenters (stars) and "stuck patches" (bars labeled I to VI) inferred to represent potential fault rupture lengths (Oppenheimer et al., 1990).

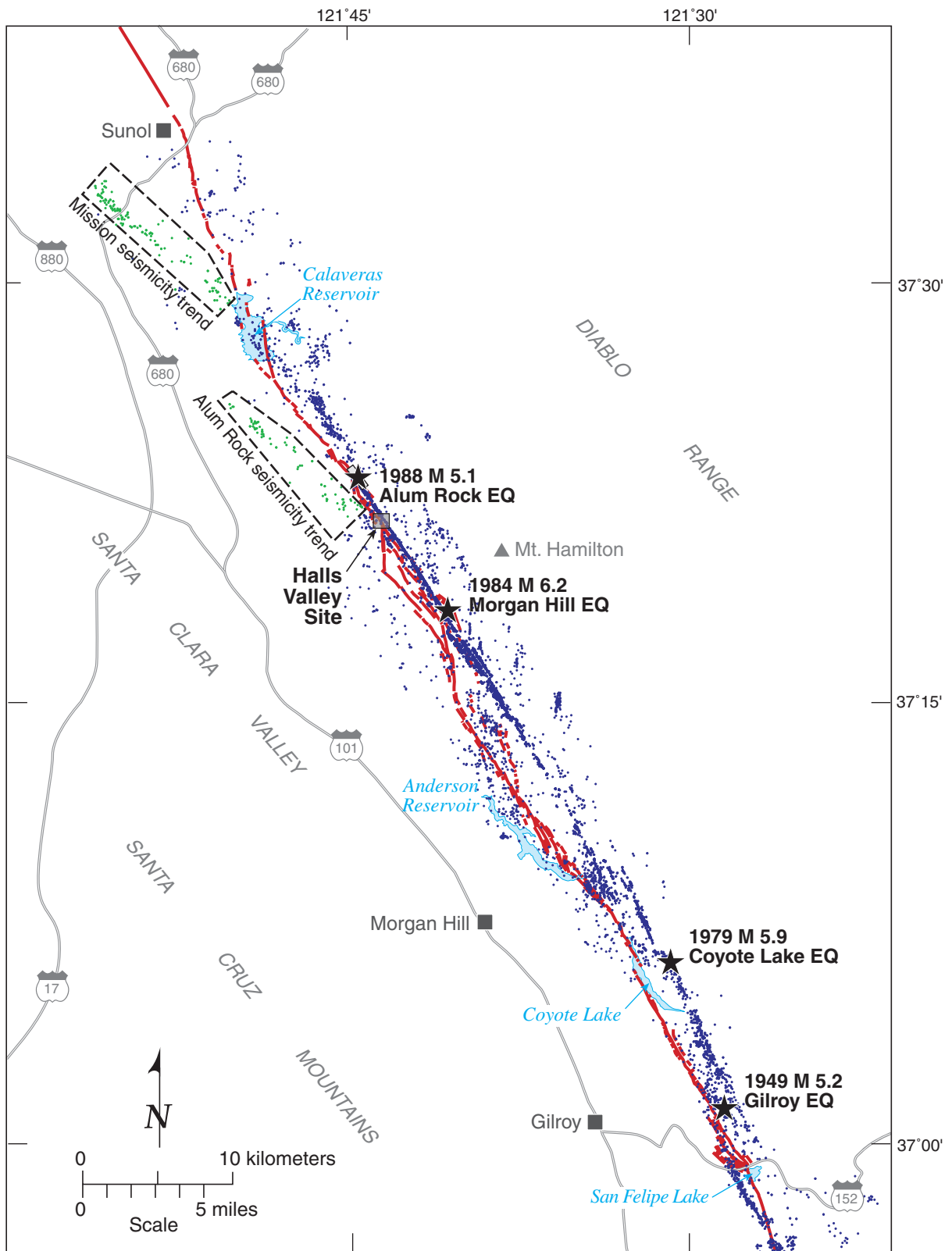


Figure 3. Map of central Calaveras fault and associated instrumental seismicity from Northern California Earthquake Data Center and Schaff et al. (2002). Historic  $M > 5$  earthquake epicenters (stars) from Oppenheimer et al. (1990). Zones of aligned seismicity shown in green include the Mission seismicity trend and the Alum Rock seismicity trend.

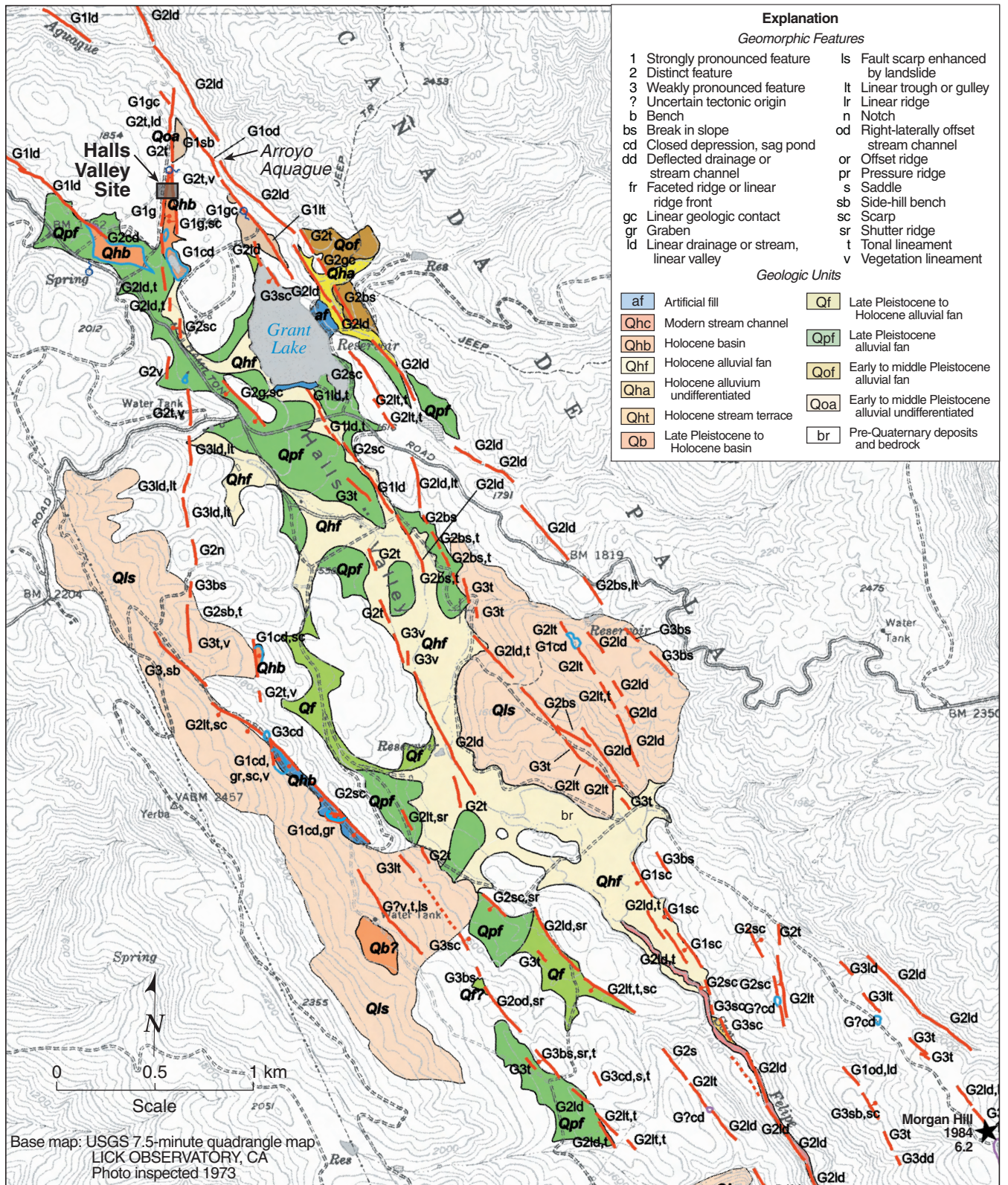


Figure 4. Quaternary geologic and geomorphic map of the central Calaveras fault at Halls Valley (Witter et al., 2003). Detailed geomorphic lineaments and possible fault-related features are annotated using abbreviated codes and indicated with red lines. Star in lower right corner shows epicenter of 1984 Morgan Hill M 6.2 earthquake. Quaternary geologic units modified from Knudsen et al. (2000).

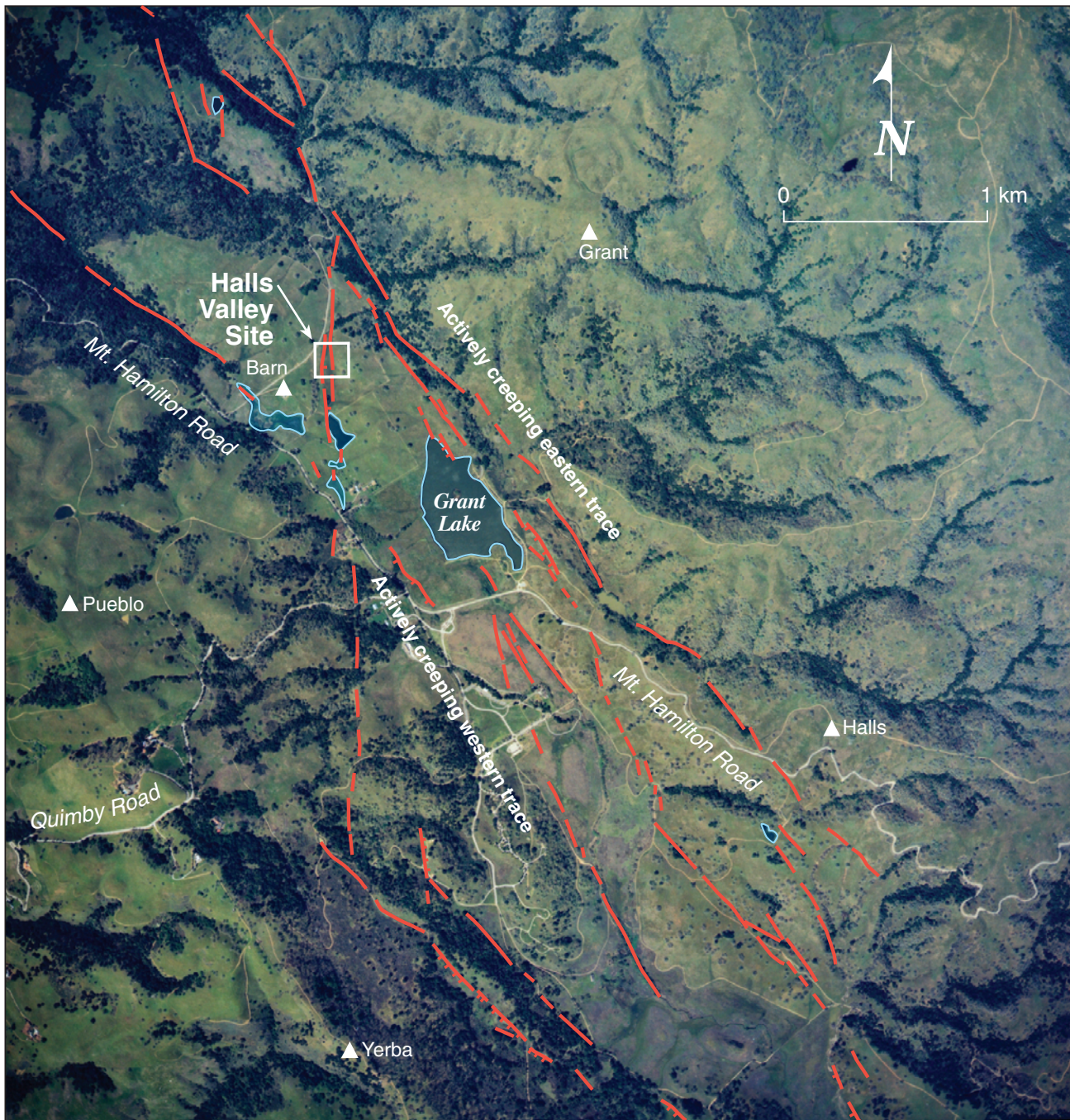


Figure 5. Interpreted aerial photograph of Halls Valley showing study site and possible fault-related geomorphic lineaments (red) and tectonic depressions (blue). Triangles show station locations of the Grant Ranch geodetic network that shows evidence for  $9.4 \pm 0$  mm/yr creep across at least two fault traces that bound the northeastern and southwestern margins of Halls Valley (Prescott et al., 1984).

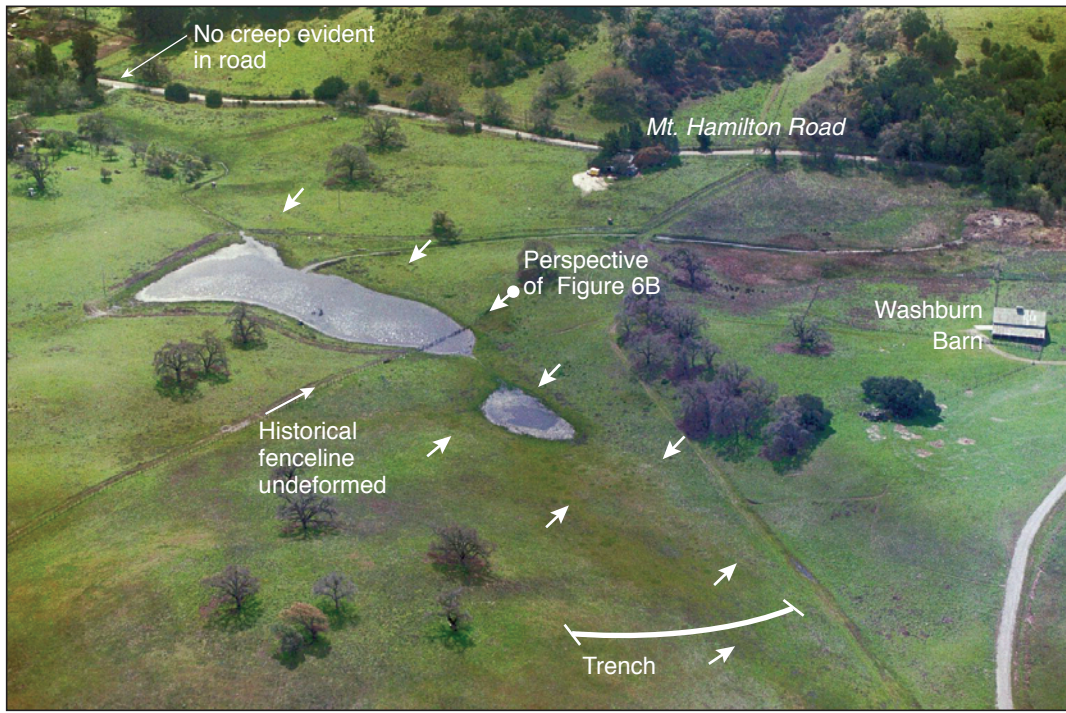


Figure 6(A). Oblique aerial photograph of trench site looking southwest showing the north trending linear trough, northwest-trending tonal lineaments (white arrows), possible tectonic depressions containing vernal ponds, and apparently undeformed historic fenceline. The Washburn Barn (far right side of photograph) marks one of five survey monuments of the Grant Ranch trilateration network (Prescott et al., 1984).



Figure 6(B). Photograph facing east that shows straight historic fenceline apparently undeformed by creep on secondary traces of the central Calaveras fault. The absence of creep evidence at this location suggests that evidence for historic creep across the Grant Ranch network is localized on primary traces of the fault to the northeast and southwest of the site.

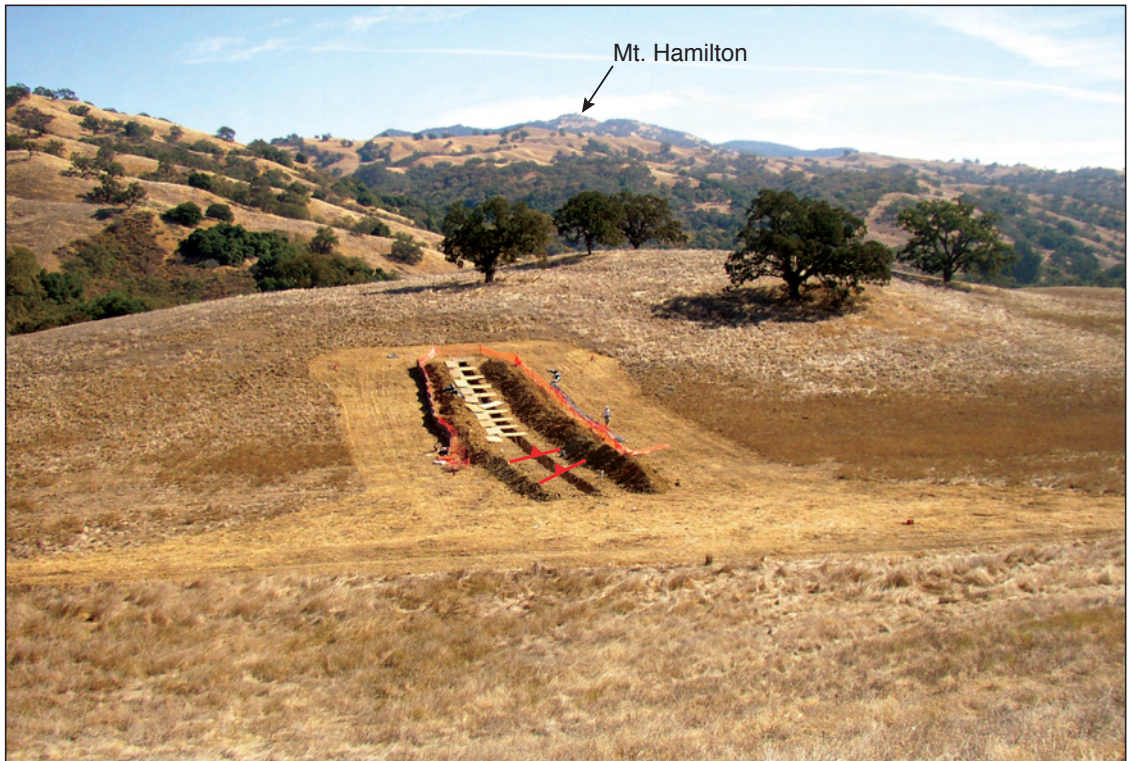


Figure 7(A). Photograph of Halls Valley trench site looking east toward Mt. Hamilton in the distance. Reverse faults exposed in the trench shown as red lines with barbs on the hanging wall.



Figure 7(B). Photograph of Halls Valley trench site looking west. Reverse faults observed in trench shown as red lines with barbs on the hanging wall.

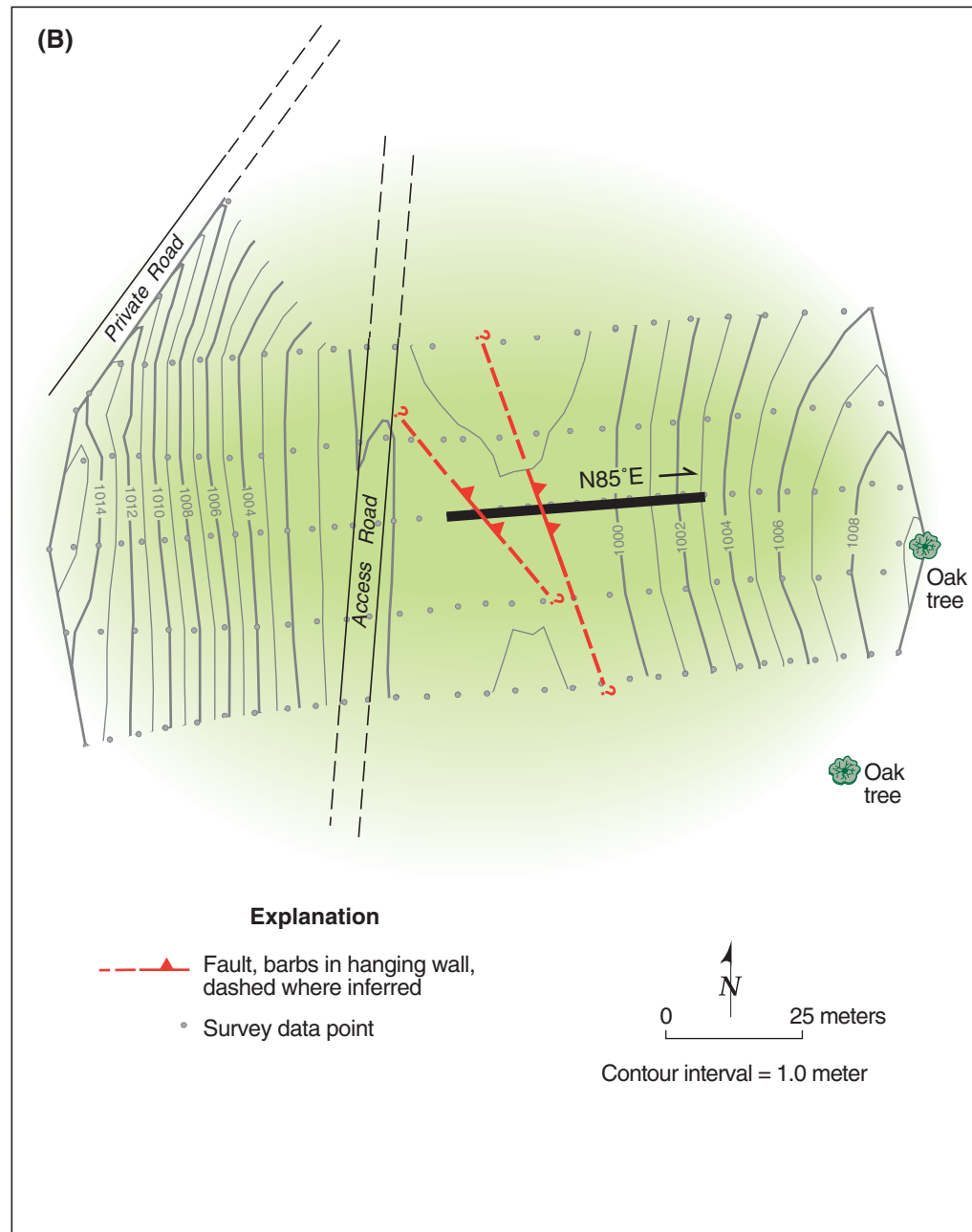
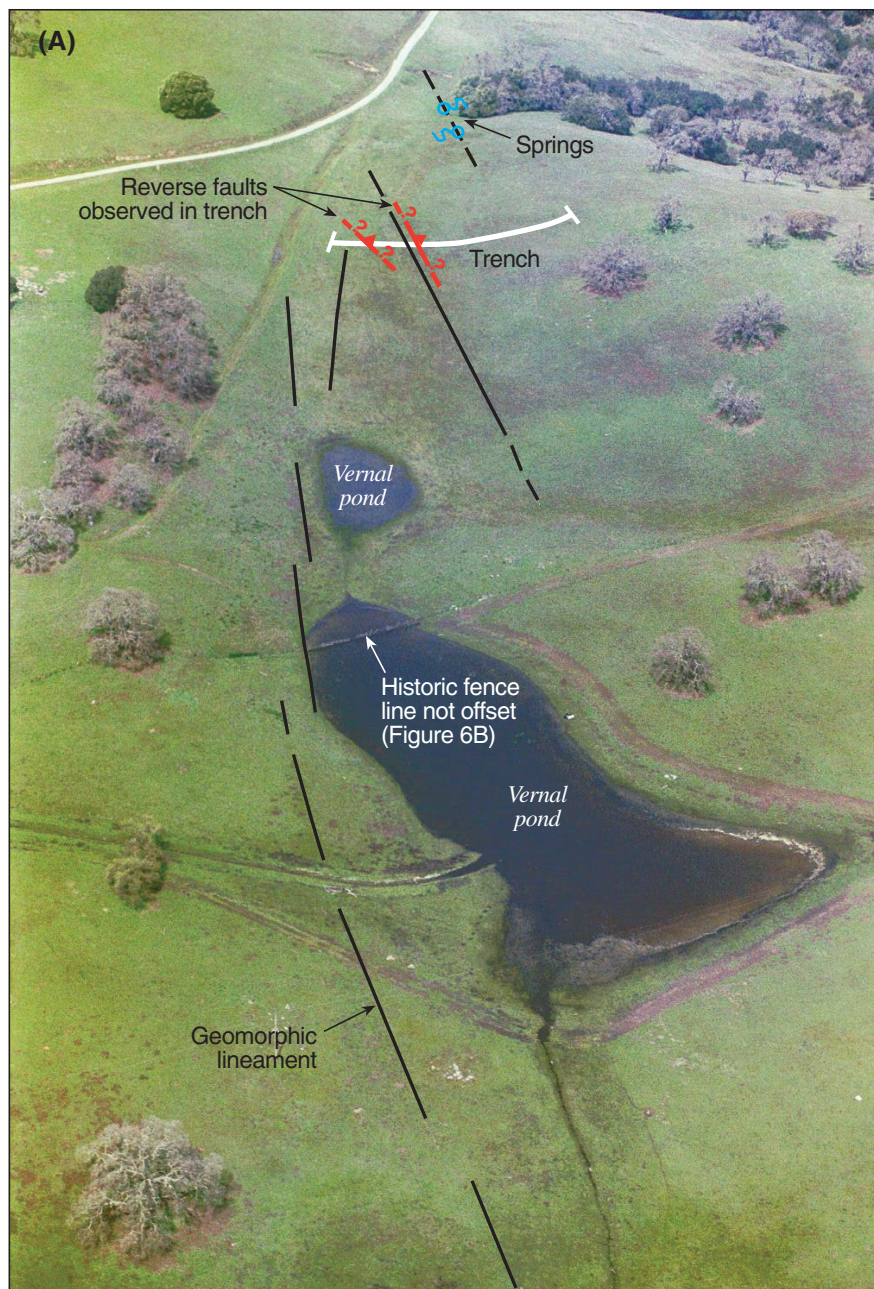
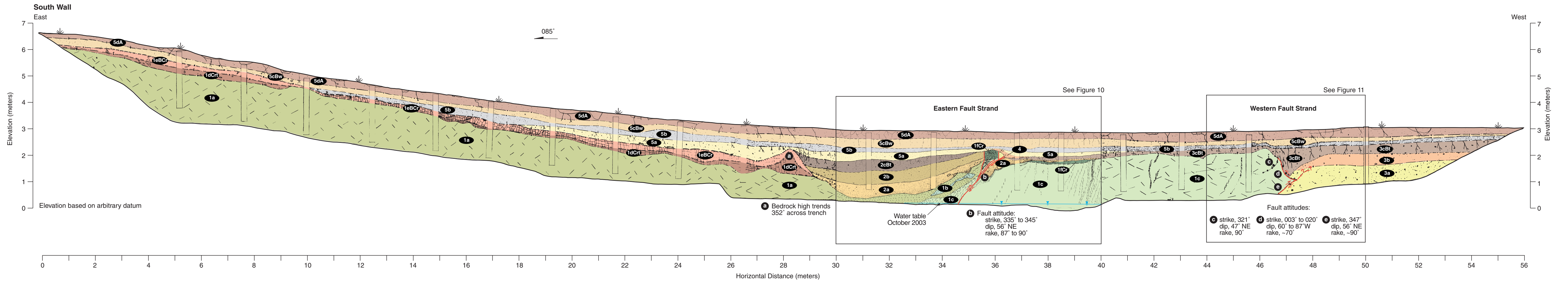
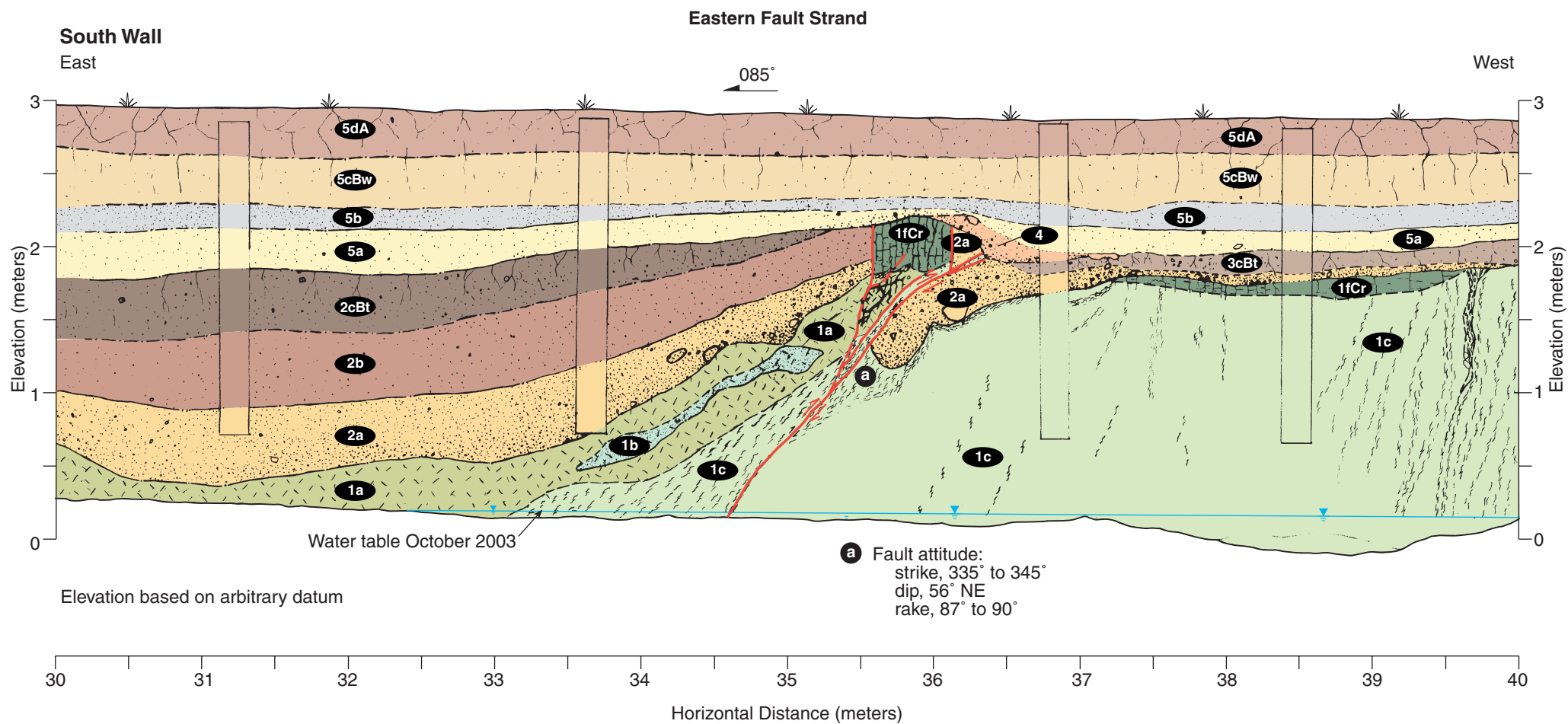


Figure 8. (A) Photograph (looking north) showing the Halls Valley trench site, northwest-trending tonal lineaments (black lines) and two vernal ponds within a north-trending linear depression. Red lines show reverse faults (barbs on the hanging wall) exposed in trench. (B) Detailed topographic map of trench site showing the orientations of two northwest-striking, northeast-dipping reverse faults observed in trench.



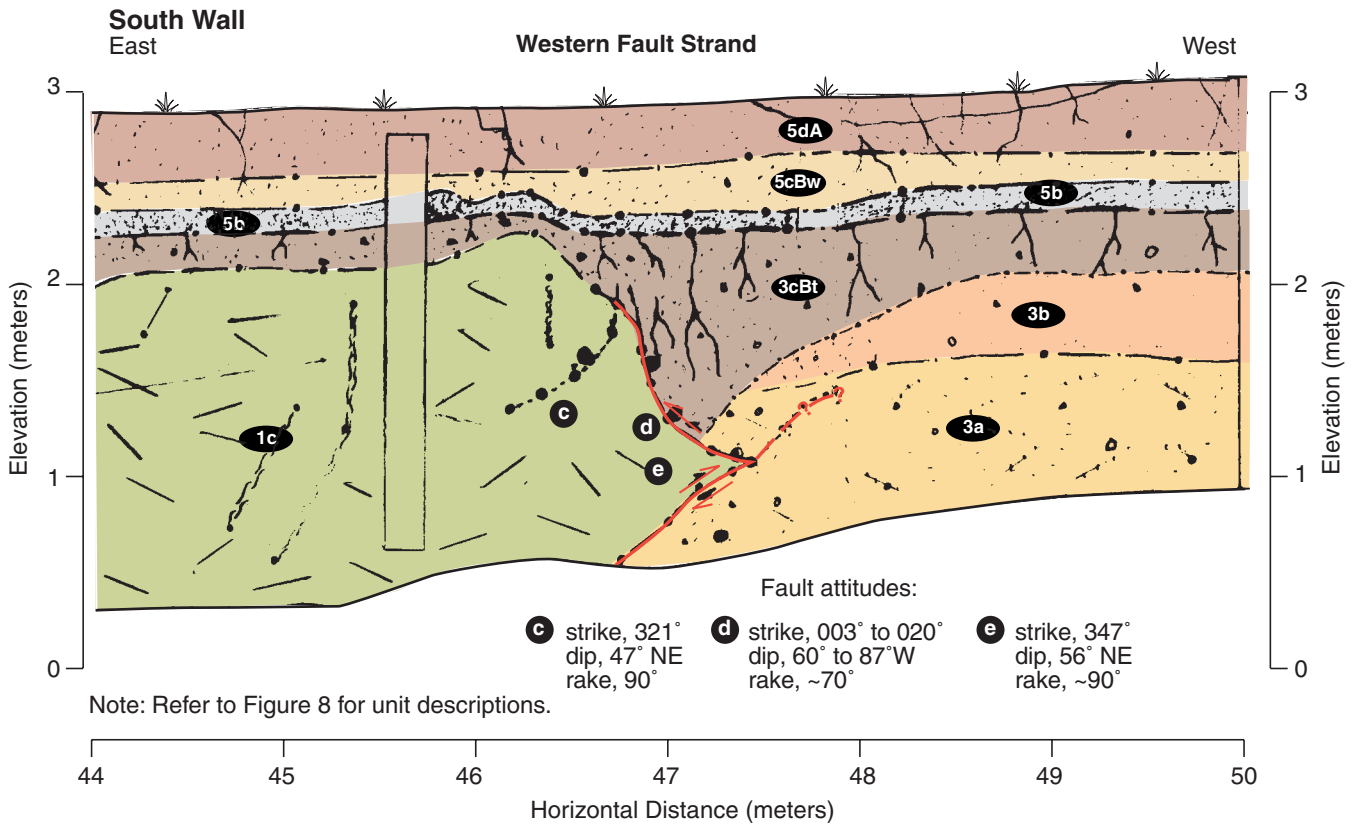
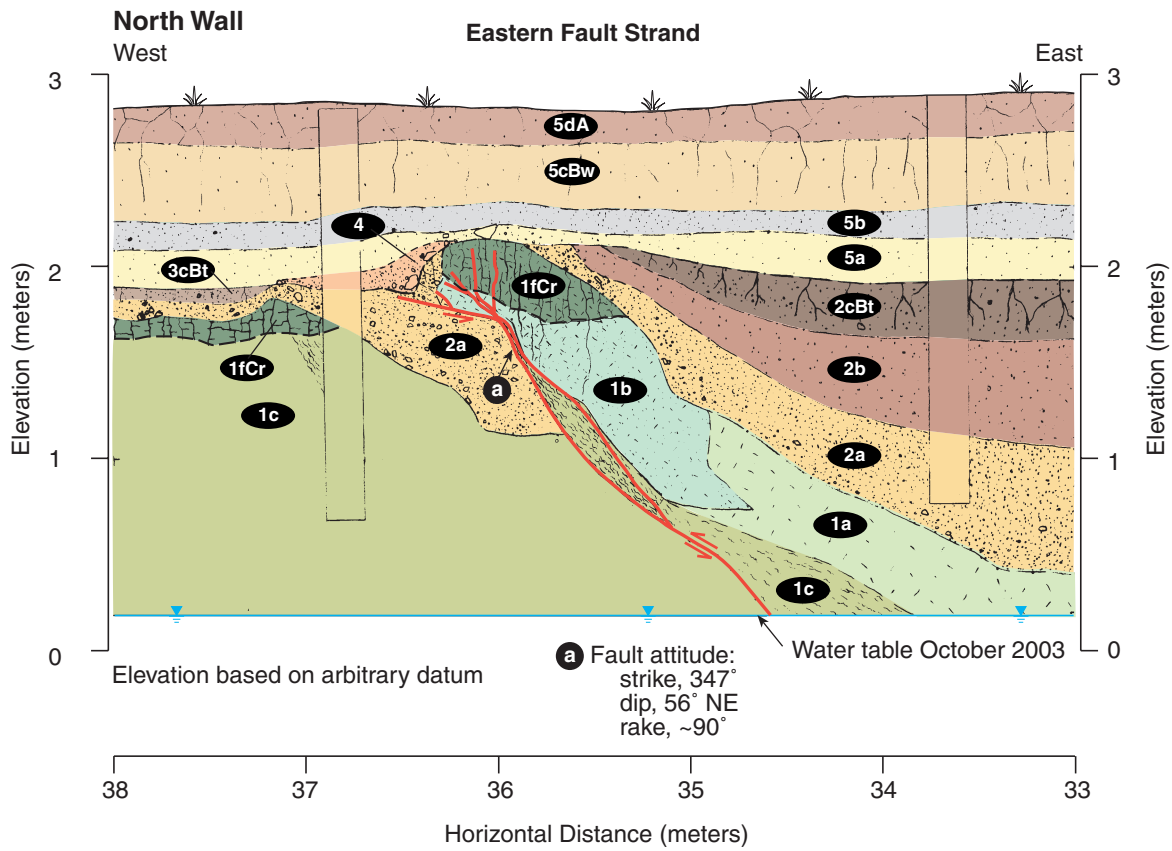
**Explanation**

Unit Descriptions	Unit Descriptions (continued)	Unit Descriptions (continued)	Symbols
<p><b>Unit 1</b>—Late Jurassic to Early Cretaceous rocks of the Franciscan Formation mélangé complex (Cotton, 1972).</p> <p><b>1a</b> Light olive-brown (2.5Y 5/4) sandstone and siltstone; oxidized, dry, medium strong, moderate to highly weathered blocky/seamy structure; rock is highly fractured and contains very minor clay seams on fracture faces. Overall no bedding is apparent, however, to the east weak west-dipping bedding planes are apparent, clay coatings on fractures are dark reddish brown (5YR 3/4).</p> <p><b>1b</b> Irregular, poorly-defined bed of massive sandstone interbedded within Unit 1a that occurs east of eastern fault strand.</p> <p><b>1c</b> Dark grey, intensely sheared, stiff to very stiff, fractured siltstone with steep, east-dipping to vertical shear fabric. Quartz veins locally parallel shear fabric; greenstone (?) chaotically distributed throughout. This unit occurs predominantly between the eastern and western fault strands.</p> <p><b>1dCr</b> Strongly weathered bedrock (sapolite) with pedogenic structure and accumulation of secondary clay and minor carbonate (Late Pleistocene (?) soil Cr-horizon). Olive-brown (2.5Y 4/4) silty clay to clay; dry, completely weathered rock, medium strong to strong, 30 to 50% angular clasts, abundant sub-horizontal to vertical pressure faces, with strong clay films on pressure faces caused by shrink-swell cycles, slickensides in all orientations; blocky prismatic pedogenic structure, rare carbonate nodules, &lt;1cm in size.</p> <p><b>1eBCr</b> Color and structural soil development in bedrock (Late Pleistocene (?) soil BCr-horizon). Strong brown (7.5YR 4/6) Silty clay, with 50 to 60% rock fragments, average rock fragment &lt;1 cm long, rare clasts 1 to 3 cm long, dry, well developed blocky columnar pedogenic structure, moderate clay films developed on ped faces.</p> <p><b>1fCr</b> Pedogenically altered bedrock (sapolite) with moderate prismatic soil structure (Latest Pleistocene to Holocene (?) soil Cr-horizon). This soil, developed locally in mélangé units, is vertically offset by the eastern fault strand. The soil formed after erosion of unit 1eBCr and subsequent bedrock exposure caused by hanging-wall uplift on the eastern and western fault strands.</p>	<p><b>Unit 2</b>—Latest Pleistocene to Holocene (?) alluvium that fills a structurally controlled paleochannel located east of the eastern fault strand.</p> <p><b>2a</b> Light yellowish brown (2.5Y 6/4) silty to sandy gravel. Gravel is massive, coarse, poorly sorted, dry, very hard. Unit consists of 45 to 55% gravel, 30% sand, 20% silt. Angular siltstone cobbles up to 5 cm in diameter. Clast lithologies include: chert, greenstone, quartz and sandstone. Bold, brown (10YR 4/3) clay films on fractures, no roots, no carbonate; sharp (within 1 cm) and wavy lower contact. Quartz clasts in gravel derived from pervasively sheared, high-grade metamorphic rocks of Franciscan mélangé in footwall of eastern fault.</p> <p><b>2b</b> Olive-yellow (2.5Y 6/6) Gravelly to silty sand. Massive, dry, hard, with dark brown clay films (7.5YR 3/2) coating subvertical fractures. Constituents include: 10 to 15% gravel, 40 to 50% fine to very fine sand, 35 to 50% silt, gravel clasts &lt;2 cm, clasts derived from weathering of local siltstone. Few 1 mm diameter roots; diffuse and smooth lower contact.</p> <p><b>2cBt</b> Brownish yellow (10YR 6/6) Gravelly to silty sand. Massive, dry, hard. Constituents include: 20 to 25% dark brown (7.5YR 3/3) translocated clay, 15 to 20% gravel; gravel clasts generally &lt;5 cm long; gradual lower contact (5 to 10 cm) is smooth.</p> <p><b>Unit 3</b>—Latest Pleistocene to Holocene (?) colluvium encountered in western part of trench.</p> <p><b>3a</b> Yellowish brown (10YR 5/4) Gravelly to silty sand. Massive, damp, stiff to very stiff, with the following constituents: 30 to 35% fine to very-fine sand, 25 to 30% silt, 25 to 30% gravel, 5 to 10% medium to coarse sand, &lt;5% clay. Subangular gravel clasts include quartz and siltstone lithologies; average clast &lt;0.5 cm long, largest clast ~2 cm long. Very weak to no pedogenic structure, few to sparse filamentous CaCO<sub>3</sub>; very weak dark brown mottles. Lower contact not observed.</p> <p><b>3b</b> Light yellowish brown (2.5Y 6/4) Gravelly to silty sand. Massive, dry, very stiff (hard), with 30 to 35% fine to very fine sand, 25 to 30% silt, 25 to 30% gravel, 5 to 10% medium to coarse sand, &lt;5% clay. Gravel is subangular with quartz clasts, average clast size &lt;0.5 cm long; largest clast 2 cm long. Moderate yellowish brown clay films (10YR 5/4) developed on soil fractures, no pedogenic structure, common &lt;1 mm-diameter pores, no roots; basal contact diffuse (5 to 10 cm) and smooth.</p> <p><b>3cBt</b> Holocene (?) strong soil Bt-horizon developed in colluvium. Light yellowish brown (2.5Y 6/4) Silty to gravelly sand. Massive, dry, hard, with 30 to 35% fine to very fine sand, 25-30% silt, 15 to 20% gravel, 5 to 10% medium to coarse sand, 10 to 20% clay. Strong, very dark grayish brown (10YR 3/2) clay films along rootlets and vertical soil fractures; basal contact diffuse (10 to 15 cm) and smooth.</p>	<p><b>Unit 4</b>—Latest Pleistocene to Holocene (?) colluvium possibly derived from fault scarp.</p> <p><b>4</b> Light yellowish brown (2.5Y 6/4) Sandy silt. Massive, dry, very stiff, with 40 to 45% silt, 40 to 45% fine to very fine sand, minor clay content, 15 to 20% gravel. Gravel clasts are subangular and likely derived from unit 10 that occurs in fault hanging wall to the east. Lower contact clear (1 to 2 cm) and smooth.</p> <p><b>Unit 5</b>—Holocene (?) colluvium.</p> <p><b>5a</b> Light yellowish brown (2.5Y 6/4) Sandy silt. Massive, dry, very stiff, with 40 to 50% silt, 40 to 50% fine to very fine sand, minor clay content, and 5 to 10% gravel. Subangular gravel clasts consist of quartz fragments and crystalline rock including metamorphosed volcanics. Thin, brown (7.5YR 4/4) clay films on pedogenic faces, poorly developed irregular blocky structure with vertical to subvertical soil fractures. Few fine root pores &lt;1 mm in diameter. Lower unconformable contact clear (over 1 to 2 cm) and smooth, and truncates Units 2a, 2b, and 2bBt.</p> <p><b>5b</b> Pale yellow (2.5Y 7/3) Silty sand. Massive, dry, very stiff, with 65% very fine sand, 25% silt, 10 to 12% angular to subangular clasts, no clay. Clasts generally &lt;2 cm in diameter, and consist of quartz and greenstone. No soil structure apparent, no clay films, no carbonate, abundant fine pores &lt;2 mm in diameter and vesicular. Light yellowish brown (10YR 6/4) weak mottles; mottles appear to be translocated clay and are diffuse. Basal erosional contact is smooth and gradual (within 3 to 5 cm).</p> <p><b>5cBw</b> Late Holocene soil Bw-horizon developed in colluvium. Yellowish brown (10YR 5/4) Sandy silt. Massive, dry, medium stiff, 20 to 40% very-fine sand, 55 to 65% silt, trace clay, 5 to 10% angular rock clasts. Clasts up to 4 cm long include quartz and siltstone lithologies. Moderately well developed, subangular blocky pedogenic structure, pedogenic blocks approximately 1cm in size, no clay films, no carbonate, abundant pores 1 to 2 mm in diameter, abundant very fine rootlets. Lower contact gradual (over 5 cm) and smooth.</p> <p><b>5dA</b> Late Holocene immature soil A-horizon, development, developed in colluvium (modern soil). Light yellowish brown (10YR 6/3) Sandy silt. Massive, dry, medium stiff to stiff, with 35 to 45% fine to very fine sand, 50% silt, 5% medium to coarse sand, &lt;5% angular rock clasts with trace clay. Clast lengths average 1 to 2 cm on long axis. Moderately developed angular blocky pedogenic structure, no clay films, no carbonate, friable structure, abundant fine and very fine rootlets and pores; lower contact diffuse over 5 to 10 cm and smooth.</p>	<p>--- Fault, dashed where inferred</p> <p>Blocky, prismatic soil structure</p> <p>Soil development</p> <p>Large pebbles, cobbles or boulders</p> <p>Shear fabric</p>



Note: Refer to Figure 8 for unit descriptions.

CENTRAL CALAVERAS FAULT ZONE HALLS VALLEY, CALIFORNIA	
<b>Detailed Log of Eastern Reverse Fault Exposed in South Wall of Trench</b>	
	William Lettis & Associates, Inc.
Figure 10	



CENTRAL CALAVERAS FAULT ZONE  
HALLS VALLEY, CALIFORNIA

**Detailed Logs of Eastern and Western Fault Strands**

WLA William Lettis & Associates, Inc. Figure 11

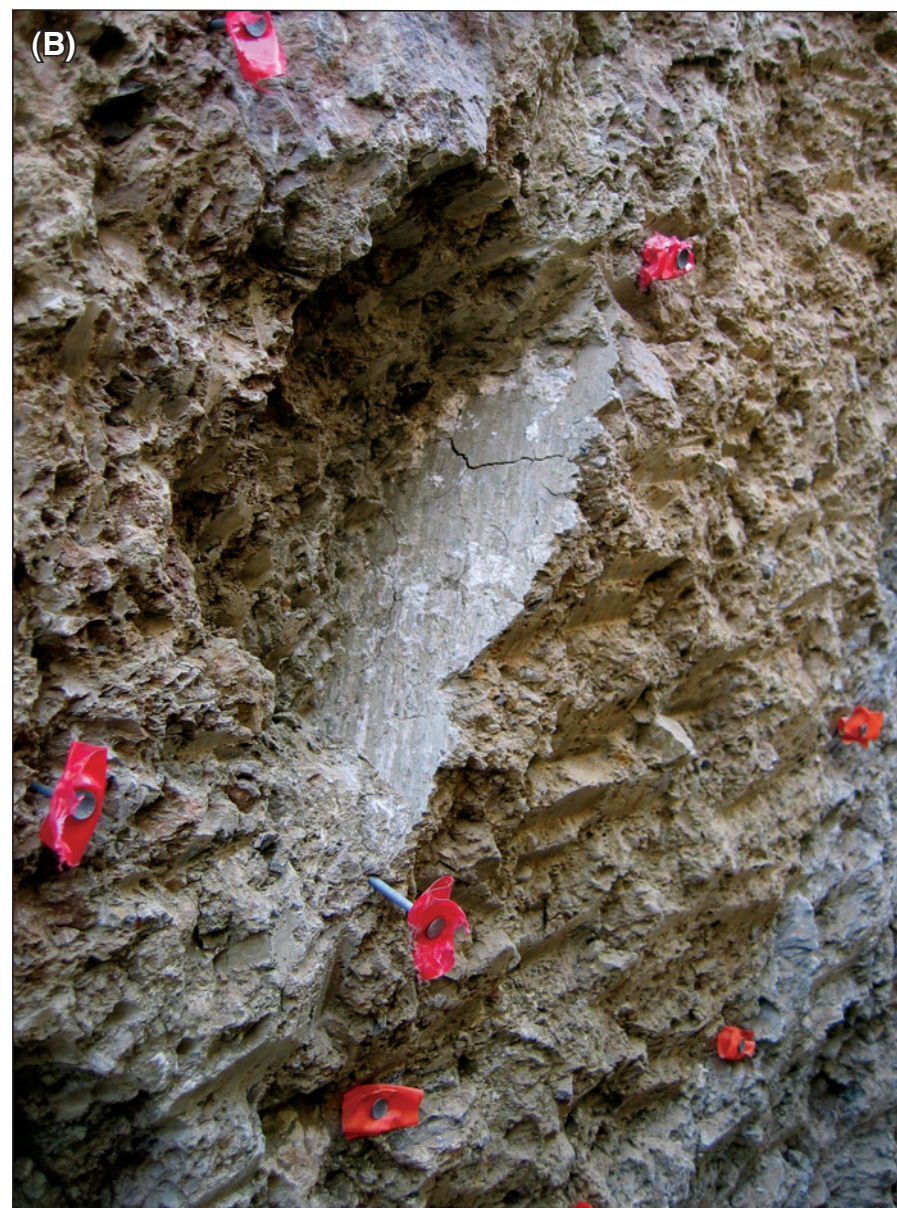


Figure 12. (A) Oblique photograph from within trench of the eastern fault strand exposed in south wall. Unit 2 alluvium is displaced in a reverse sense to the west over Franciscan Complex bedrock. (B) Closeup photograph showing slickensides on fault plane. Striations on the fault plane indicate pure reverse dip-slip motion.

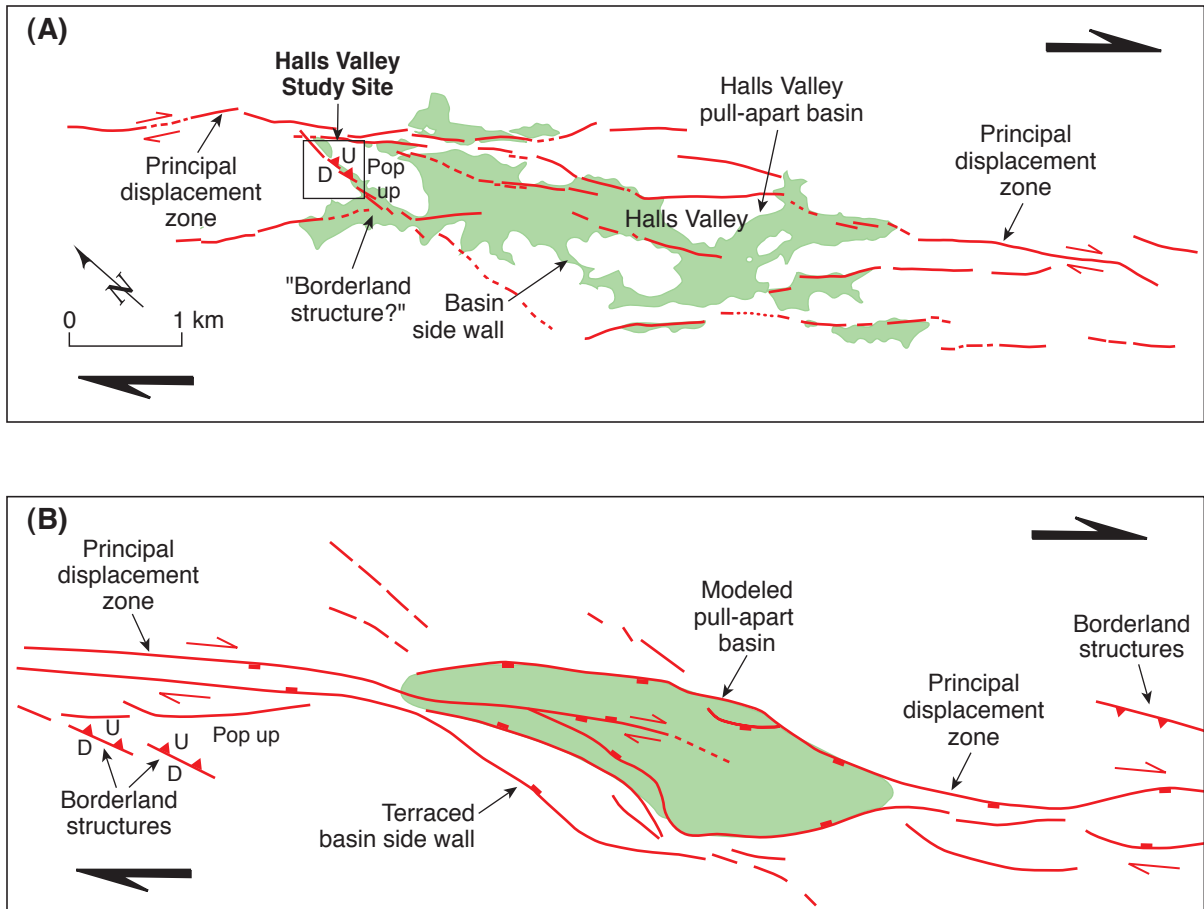


Figure 13. (A) Map of fault-related geomorphic lineaments that define a right-releasing stepover along the central Calaveras fault at Halls Valley. Green area delineates extent of pull-apart basin based on the distribution of Pleistocene and younger deposits. (B) Interpreted map of faults and pull-apart basin (green area) formed by a scaled sandbox experiment designed to model releasing stepovers along strike-slip faults (Dooley and McClay, 1997).